Chapter 4

The Seasonal Cycle of Sea Level Along the Coast

There are four causes of the climatological seasonal cycle of coastal sea level (Section 2.2). Of these four, low-frequency astronomic tides are ignored because they force an oscillation with a range less than 1 cm, much less than the observed variability, and the effect of atmospheric pressure is removed using the Inverse-Barometer (IB) approximation. The seasonal cycle of observed and corrected sea level[1] is plotted in Figure 4.1. The corrected seasonal cycle must be forced by the two remaining processes, which together force changes in steric sea level: wind-forced coastal currents and thermohaline effects due to surface fluxes and horizontal advection of heat and salt. In this chapter, we examine the effect of these two processes within the framework of a reduced-gravity model.

4.1 Effect of Wind-Forced Coastal Currents

The $1\frac{1}{2}$-layer reduced-gravity model used in Chapter 3 is successful in simulating the major observed features of the basin-scale circulation in the north Indian Ocean. It is also able to simulate the seasonal cycle of coastal currents off India (Figure 4.2). Except at Colombo, where the ship drifts are affected more by the strong local winds than by currents[2], the model alongshore currents are in excellent agreement with the observations. This leads us to believe that the model should be able to capture the effect of these large-scale coastal currents, one of the two processes left on eliminating astronomic tides and atmospheric pressure, on sea level along the coast of India.

The model sea level is compared with corrected sea level in Figure 4.3; there is a striking

[1] Observed sea level is the measured sea level; corrected sea level is the sea level corrected for the effect of atmospheric pressure.

[2] See Figures 2.6 and 2.8.

Figure 4.1 The climatological seasonal cycle of sea level (cm) along the coast of India. The figure shows the observed and corrected sea level; the local annual mean has been subtracted from the monthly climatology to compute these anomalies. The correction for atmospheric pressure was applied using the Inverse-Barometer approximation. The effect of atmospheric pressure on sea level varies from 3 cm at Colombo to 13 cm at Paradip. The seasonal cycle of corrected sea level is coherent along the coast. Its range is greater along the east coast (45 cm) than along the west coast (30 cm). Along the east (west) coast, the corrected sea level is maximum in November (December) and minimum during March–April (the southwest monsoon).

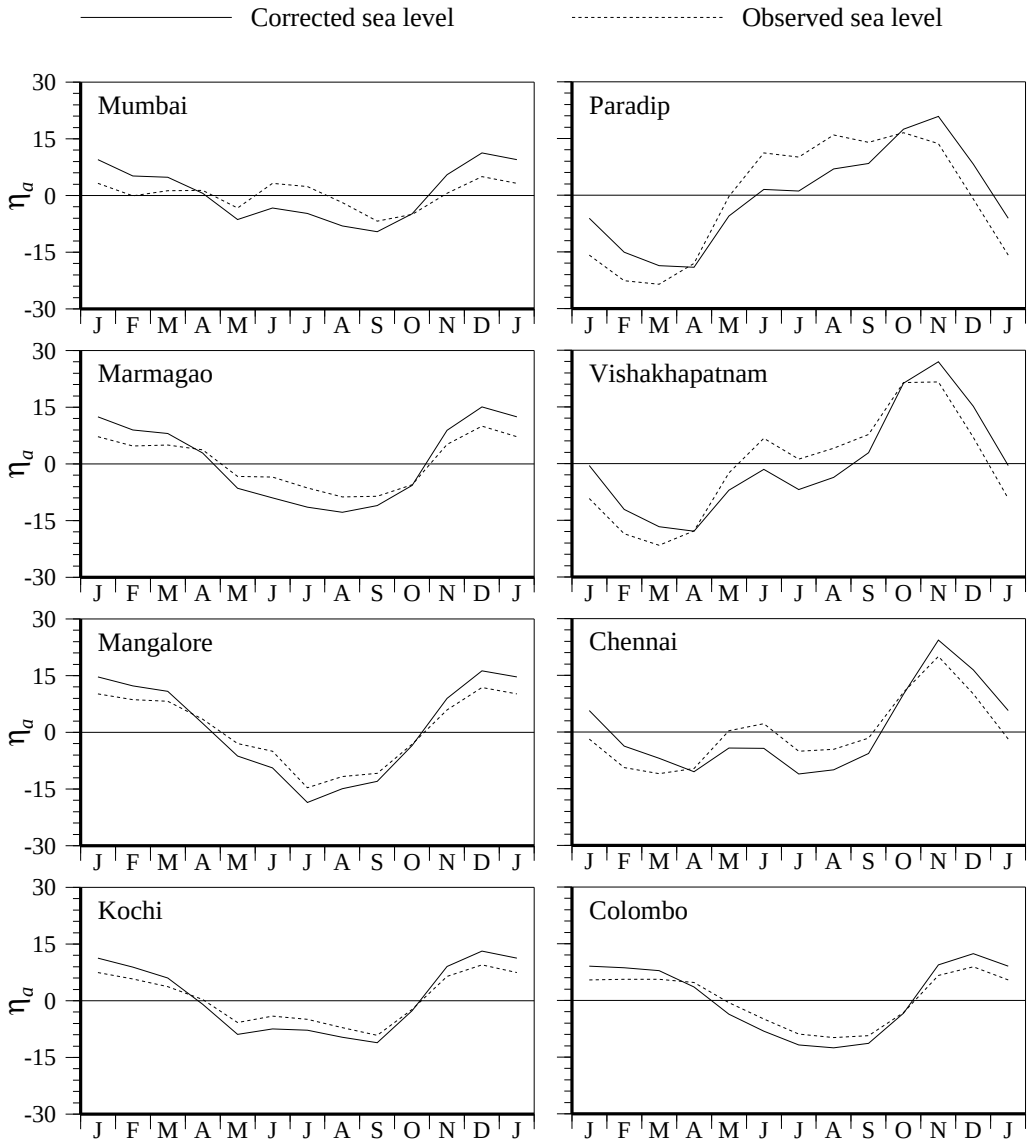

Figure 4.2 The climatological seasonal cycle of alongshore ship drifts, compiled by Rao et al. [1989] (cm s^{-1}), and alongshore currents (cm s^{-1}), simulated by the dynamical $1\frac{1}{2}$-layer reduced-gravity model. Ship-drift data are not available at Paradip and Mumbai. All variables plotted are monthly anomalies; the annual mean has been removed. Downwelling- (upwelling-) favourable anomalies are positive (negative); these currents flow with the coast on their right (left) in the northern hemisphere. The model alongshore currents match the ship drifts, except at Colombo, where the ship drifts are affected more by the strong local winds than by currents (see Figure 2.8).

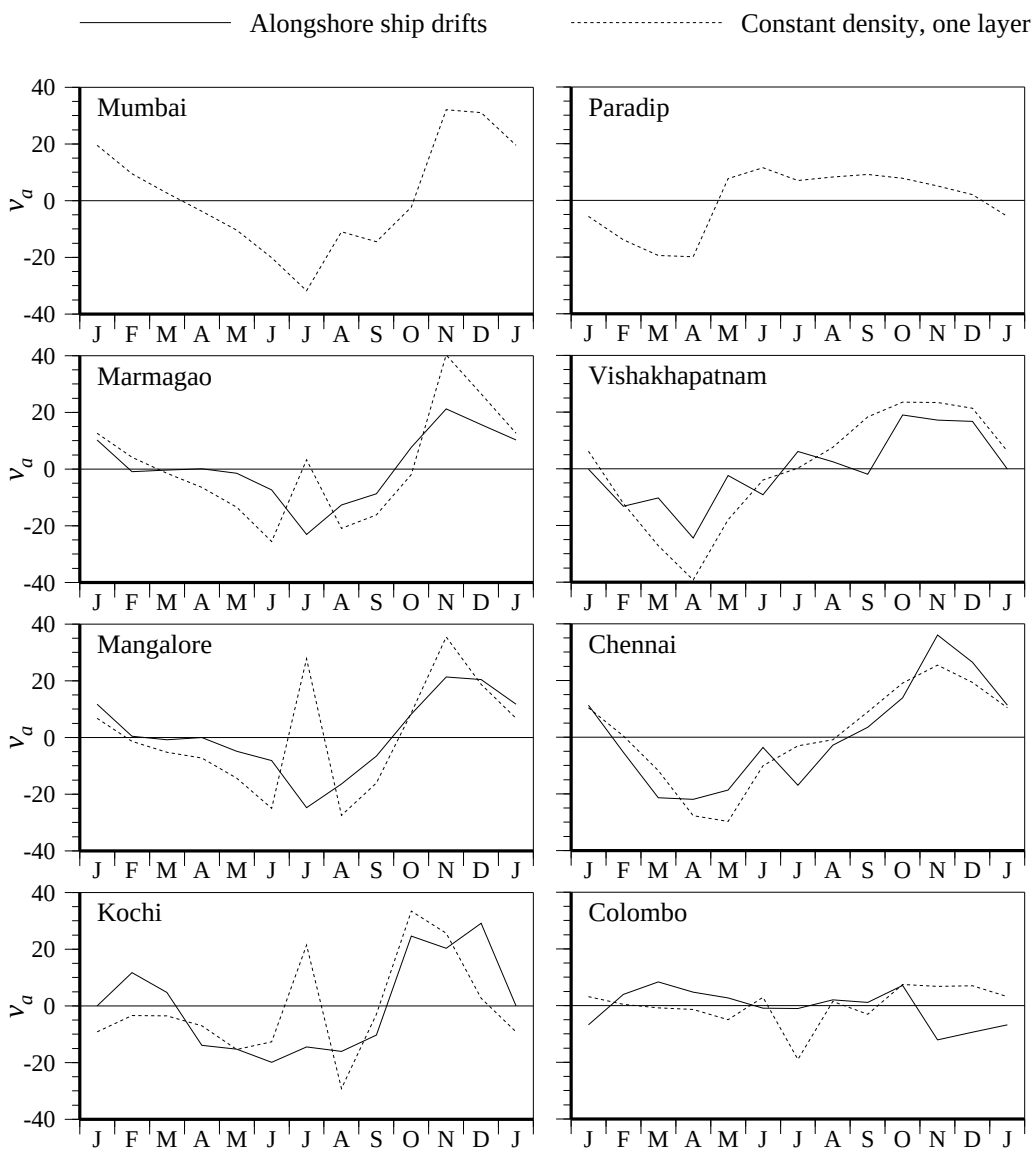

Figure 4.3 Effect of wind-forced coastal currents on the seasonal cycle of sea level (cm). Monthly anomalies of corrected sea level are plotted along with that of the sea level from the $1\frac{1}{2}$-layer and $2\frac{1}{2}$-layer models. The dynamical reduced-gravity model is successful in simulating the seasonal cycle of currents along the coast of India, but it fails to simulate that of sea level. The model fails to simulate the winter peak along the east coast; as a consequence, the simulated seasonal cycle of sea level has a higher range along the west coast.

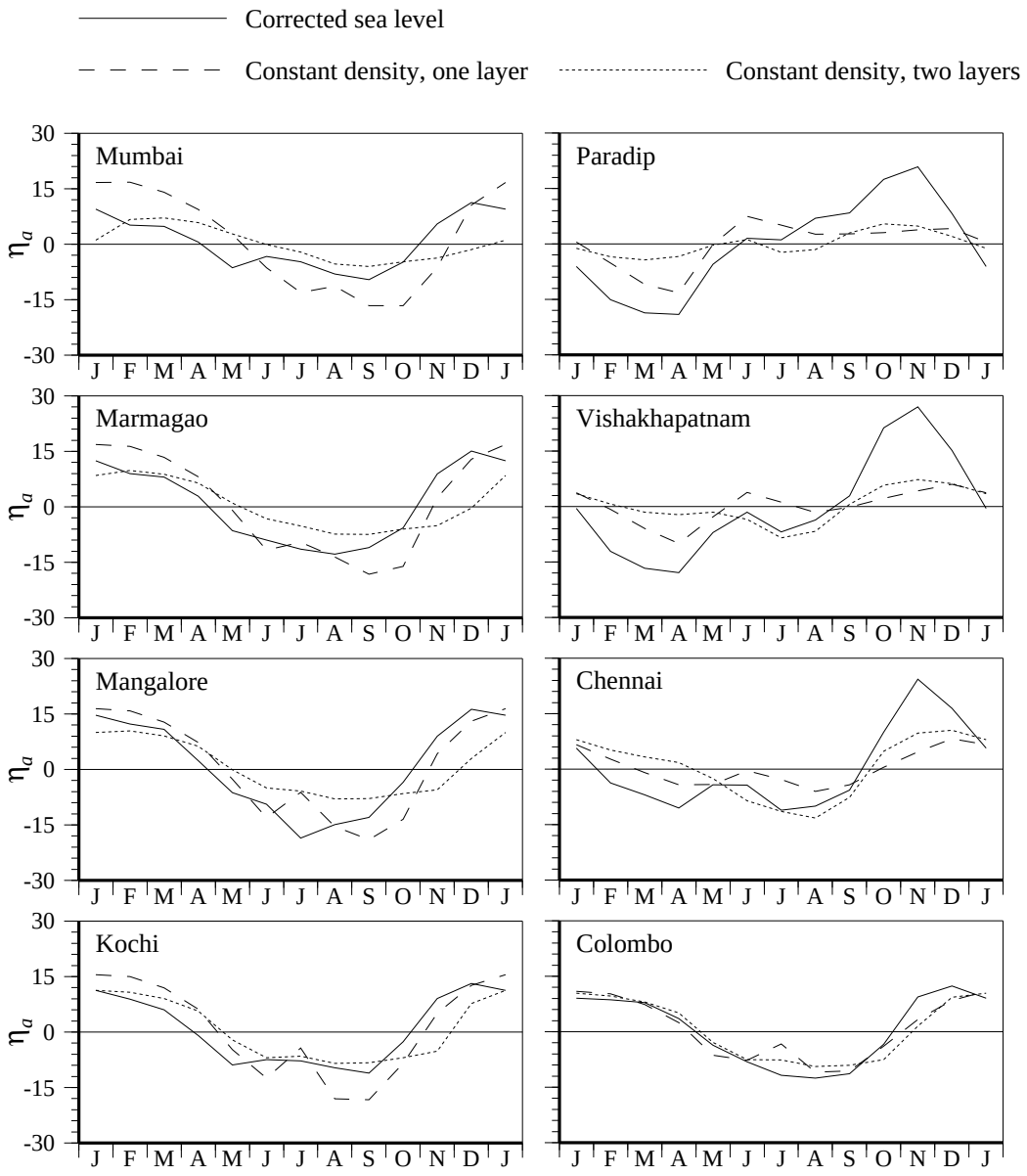

mismatch between the two, especially along the east coast. First, the model is unable to capture the winter peak along the east coast. Second, as a consequence of this, the range of the seasonal cycle along the east coast is much less than that along the west coast.

This failure implies that the model lacks the physics required to simulate the seasonal cycle of coastal sea level. Could this be due to the absence of a second active layer? The available literature suggests that the second baroclinic mode is important in the Indian Ocean, especially in the equatorial waveguide [McCreary et al., 1993; Jensen, 1993]. To examine its effect on coastal sea level, we add an extra active layer to the model, making it a $2\frac{1}{2}$-layer model[3]. The model parameters are listed in Table 4.1. Density is constant in each layer and the model is forced by the wind-stress climatology of Hellerman and Rosenstein [1983]. The model sea level plotted in Figure 4.3 is from the tenth year of the simulation.

Table 4.1 Model parameters for the $2\frac{1}{2}$-layer reduced-gravity model.

Parameter (units)	Symbol	Value
Laplacian mixing coefficient for momentum ($cm^2\ s^{-1}$)	ν	5×10^7
Laplacian mixing coefficient for thickness ($cm^2\ s^{-1}$)	κ	1×10^7
Reduced-gravity parameter for the first layer	$\overline{\Gamma}_1$	0.0035
Reduced-gravity parameter for the second layer	$\overline{\Gamma}_2$	0.0020
Initial thickness of the first layer (m)	$\overline{H}_1$	70
Initial thickness the second layer (m)	$\overline{H}_2$	250
Minimum thickness of the first layer (m)	$H_{1,\min}$	10
Maximum thickness of the first layer (m)	$H_{1,\max}$	140
Minimum thickness of the second layer (m)	$H_{2,\min}$	50
Maximum thickness of the second layer (m)	$H_{2,\max}$	450
Grid size (km)	$\Delta x, \Delta y$	55
Time step (minutes)	Δt	72

The $2\frac{1}{2}$-layer model also fails to capture the observed variability, doing no better than the $1\frac{1}{2}$-layer model in simulating the winter peak along the east coast. This failure of the purely wind-forced reduced-gravity models to simulate the seasonal cycle of corrected sea level, even though they are able to simulate that of the alongshore currents, implies that a critical element is missing in these dynamical models. We explore if thermohaline effects constitute this critical element.

[3]The equations are derived in Appendix A; see Section A.2.

Figure 4.4 Effect of temperature on the seasonal cycle of sea level (cm). Monthly anomalies of corrected sea level are plotted along with that of the sea level from the $2\frac{1}{2}$-layer model of McCreary et al. [1993]. Like the dynamical reduced-gravity models, this too fails to simulate the winter peak along the east coast. Since the model does fairly well in simulating the temperature in the upper ocean, this failure implies that seasonal variations in temperature have a minor effect on sea level along the coast of India.

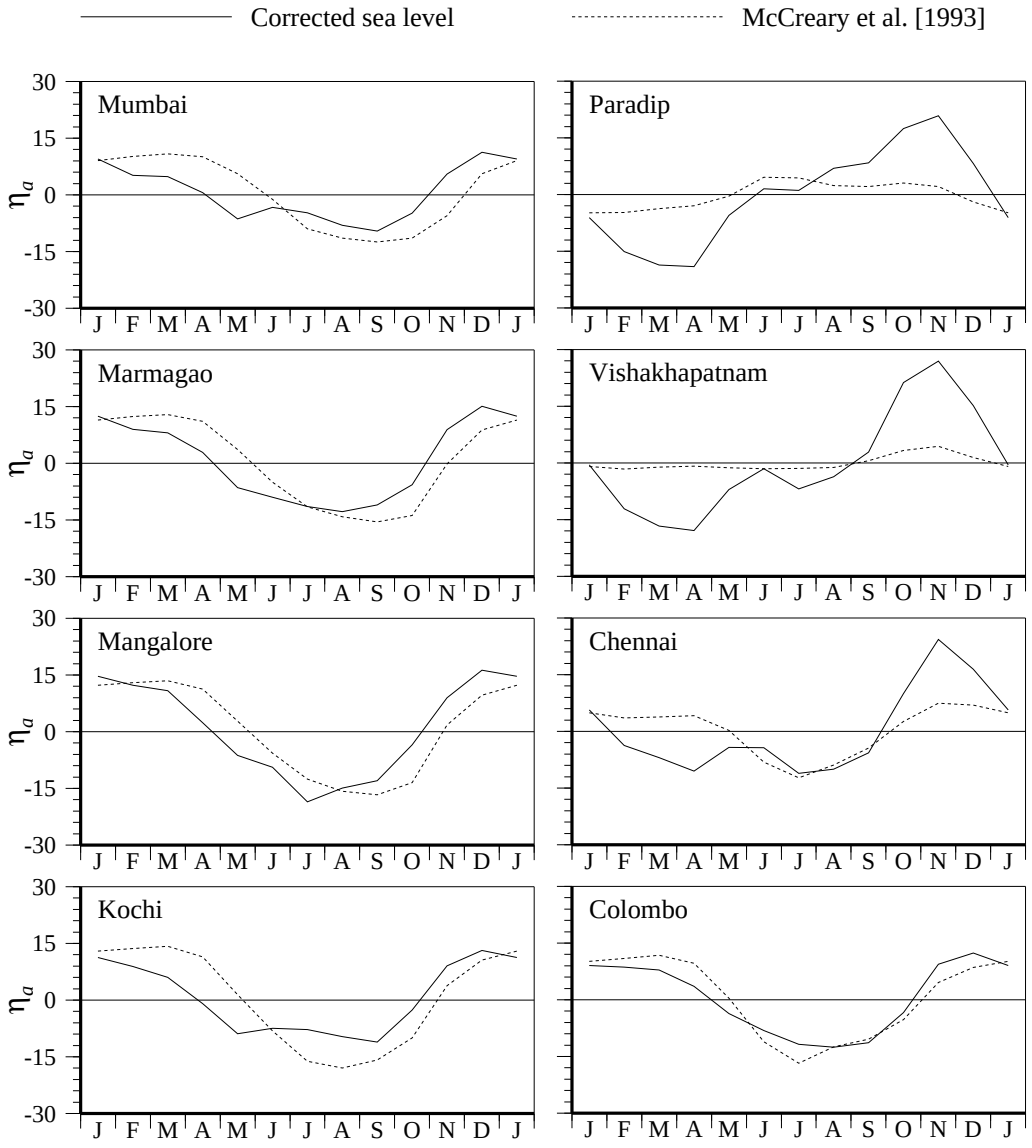

4.2 Effect of Variations in Temperature

In their numerical study of the dynamics and thermodynamics of the Indian Ocean, McCreary et al. [1993] used a $2\frac{1}{2}$-layer reduced-gravity model with a mixed layer embedded in the upper layer. The model, forced by the wind-stress climatology of Hellerman and Rosenstein [1983] and observed surface fluxes of heat, simulates the major features of the observed circulation and sea surface temperature (SST) fairly well. Hence, we expect it to account for the effect of temperature on coastal sea level. It, however, fares no better than the purely wind-forced models (Figure 4.4), implying that temperature changes play but a minor role in forcing seasonal sea-level changes along the Indian coast.

This result, which is not surprising because seasonal variations in temperature are small in the tropics [Clarke and Liu, 1993], leaves us with salinity as the possible cause of the winter peak in sea level along the east coast of India. Since the haline contraction coefficient is roughly five times the thermal expansion coefficient (Table 3.1), a salinity change of 1 PSU is equivalent to a temperature change of 5°C. Though a 5°C change in temperature is not common in the north Indian Ocean, a 1 PSU change in salinity is. The annual mean temperature and salinity, averaged over the top 100 m of the water column, and $\overline{\Gamma}$, are plotted in Figures 4.5, 4.6, and 4.7. The alongshore changes in temperature are small, but there is a large alongshore salinity gradient. Hence, salinity may be a significant cause of the seasonal cycle of sea level along the coast of India.

Figure 4.5 Annual mean temperature (°C), averaged over the top 100 m of the water column, in the north Indian Ocean. The temperature field is from the annual climatology of Levitus and Boyer [1994] and has been interpolated to the model grid.

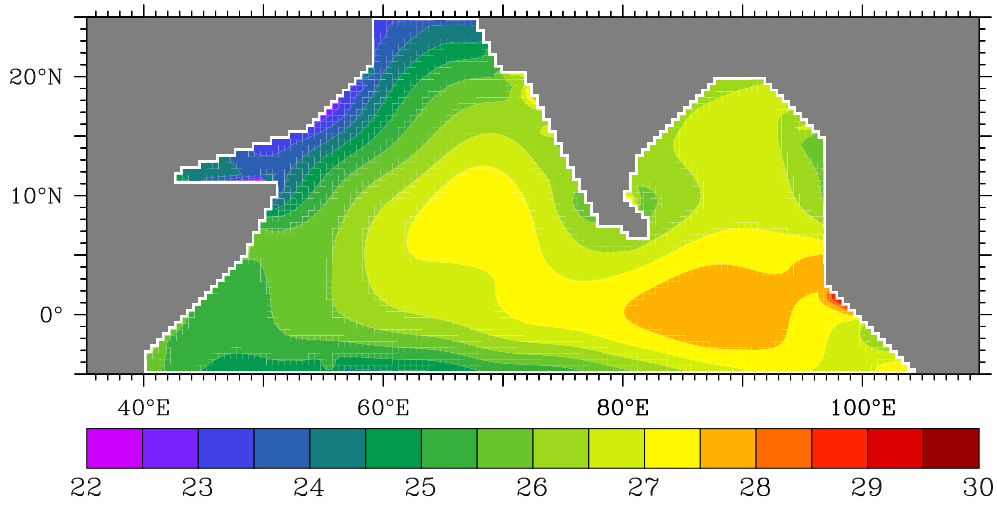

Figure 4.6 Annual mean salinity (PSU), averaged over the top 100 m of the water column, in the north Indian Ocean. The salinity field is from the annual climatology of Levitus et al. [1994] and has been interpolated to the model grid.

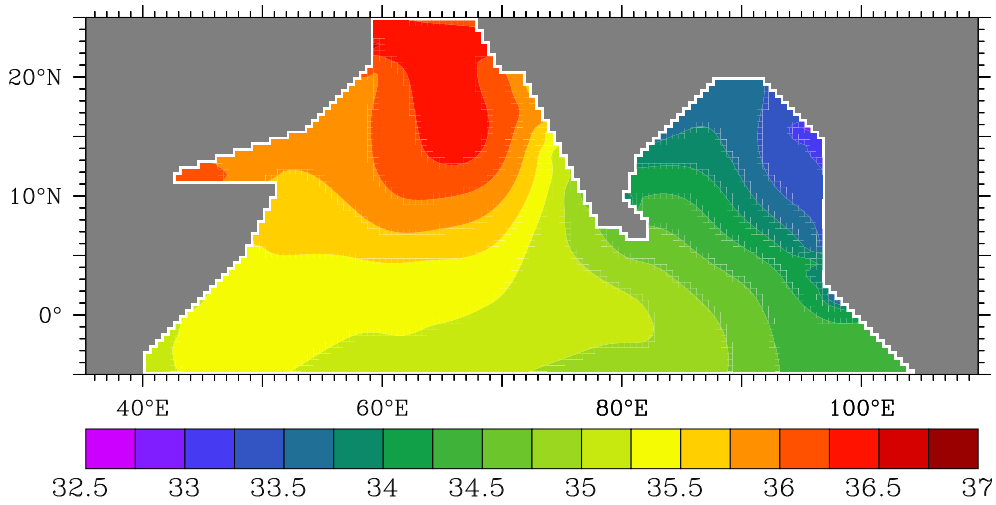

Figure 4.7 Annual mean reduced-gravity parameter $\Gamma = \frac{\rho_2 - \rho_1}{\overline{\rho}}$ in the north Indian Ocean. $\overline{\rho}$ is an average density representative of the ocean (see Appendix A). The temperature field is from the annual climatology of Levitus and Boyer [1994], the salinity field from that of Levitus et al. [1994].

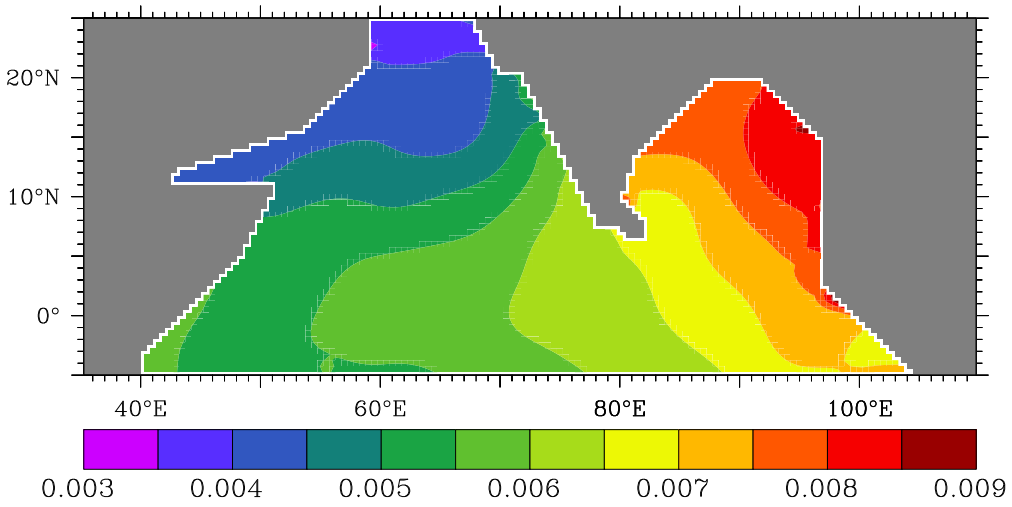

4.3 Effect of Variations in Salinity

The heavy rainfall over the Indian subcontinent leads to a large runoff from rivers into the seas around India, particularly the Bay of Bengal. Together with the rainfall over the ocean, the fresh-water inflow from rivers lowers salinity in the bay, especially along the coast of India. The low salinity is bound to raise the steric sea level along the coast.

4.3.1 Simulations With the Salinity Climatology of Levitus et al. [1994]

To examine the impact of salinity on the seasonal cycle of sea level along the Indian coast, we have to permit temperature and salinity to vary in the active upper layer of the $1\frac{1}{2}$-layer model. We do not solve the conservation equations for heat and salt[4]; instead, temperature and salinity are prescribed from the monthly climatologies of Levitus and Boyer [1994] and Levitus et al. [1994]. These monthly fields are averaged over the top 100 m and then interpolated linearly to the model grid at each time-step. The density in the upper layer is still less than that of the constant-density lower layer, but it is now a function of space and time. The resulting seasonal cycle of the reduced-gravity parameter, Γ, is plotted in Figures 4.8 and 4.9. The seasonal cycle of Γ is determined primarily by the changes in salinity in the Bay of Bengal; variations in temperature are important only in the northern Arabian Sea, where cooling by the cold continental winds blowing from the northeast in winter forces a drop in temperature in the upper ocean [Banse, 1984, 1994; Madhupratap et al., 1996], and along the west coast of India during the southwest monsoon, when Γ decreases owing to a decrease in the average temperature of the upper layer due to upwelling associated with the Lakshadweep low.

The model is forced by the wind-stress climatology of Hellerman and Rosenstein [1983] and the resulting sea-level deviation, η, and velocity, $\mathbf{v}$, are shown in Figure 4.10. The variations in density do not perturb the basin-scale circulation much. The alongshore currents also do not change much (Figure 4.11). The range of the seasonal cycle of sea level increases at Paradip (Figure 4.12), but the maximum occurs in June; at Vishakhapatnam and Chennai, there is little change in sea level. This is due to the seasonal cycle of Γ (Figure 4.9), which has a trough in November along the east coast because the coastal salinity in the climatology of Levitus et al. is minimum in September and increases thereafter. This drop in Γ lowers sea level at the coast in November even though the EICC favours downwelling, the effect of the wind-forced rise in sea level being nullified by the rise in salinity.

The monthly climatologies of Levitus and Boyer and Levitus et al. are derived from their seasonal climatologies by interpolation. The sparse distribution of the data in the north Indian Ocean makes it difficult to prepare a monthly climatology. Another problem is the absence of

[4]The equations for this variable-density reduced-gravity model are derived in Appendix A.

Figure 4.8 The seasonal cycle of the reduced-gravity parameter Γ in the north Indian Ocean. Γ is computed from the monthly climatologies of Levitus and Boyer [1994] and Levitus et al. [1994]. There is a large difference in density between the northern Bay of Bengal and the northern Arabian Sea. This difference is determined mainly by the difference in salinity [Shetye, 1984], there being a continuous increase (decrease) in salinity (Γ) from the bay to the Arabian Sea.

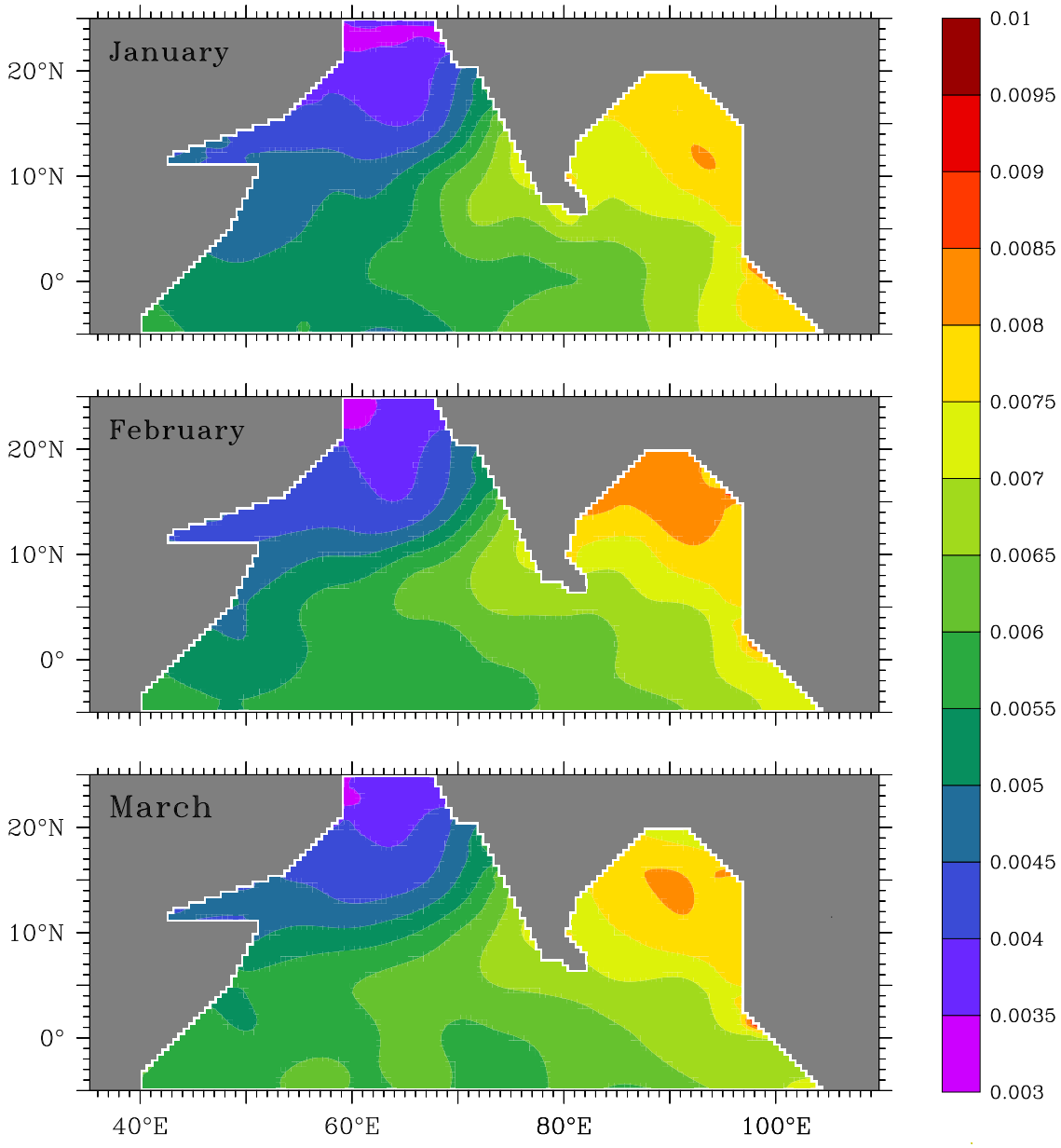

Figure 4.8 (continued) The seasonal cycle of the reduced-gravity parameter Γ in the north Indian Ocean. Γ is computed from the monthly climatologies of Levitus and Boyer [1994] and Levitus et al. [1994]. Γ does not change much during January–May. It drops during the southwest monsoon along the west coast of India because of a decrease in temperature due to upwelling associated with the Lakshadweep low. In June, it starts increasing in the northern Bay of Bengal because of a decrease in salinity.

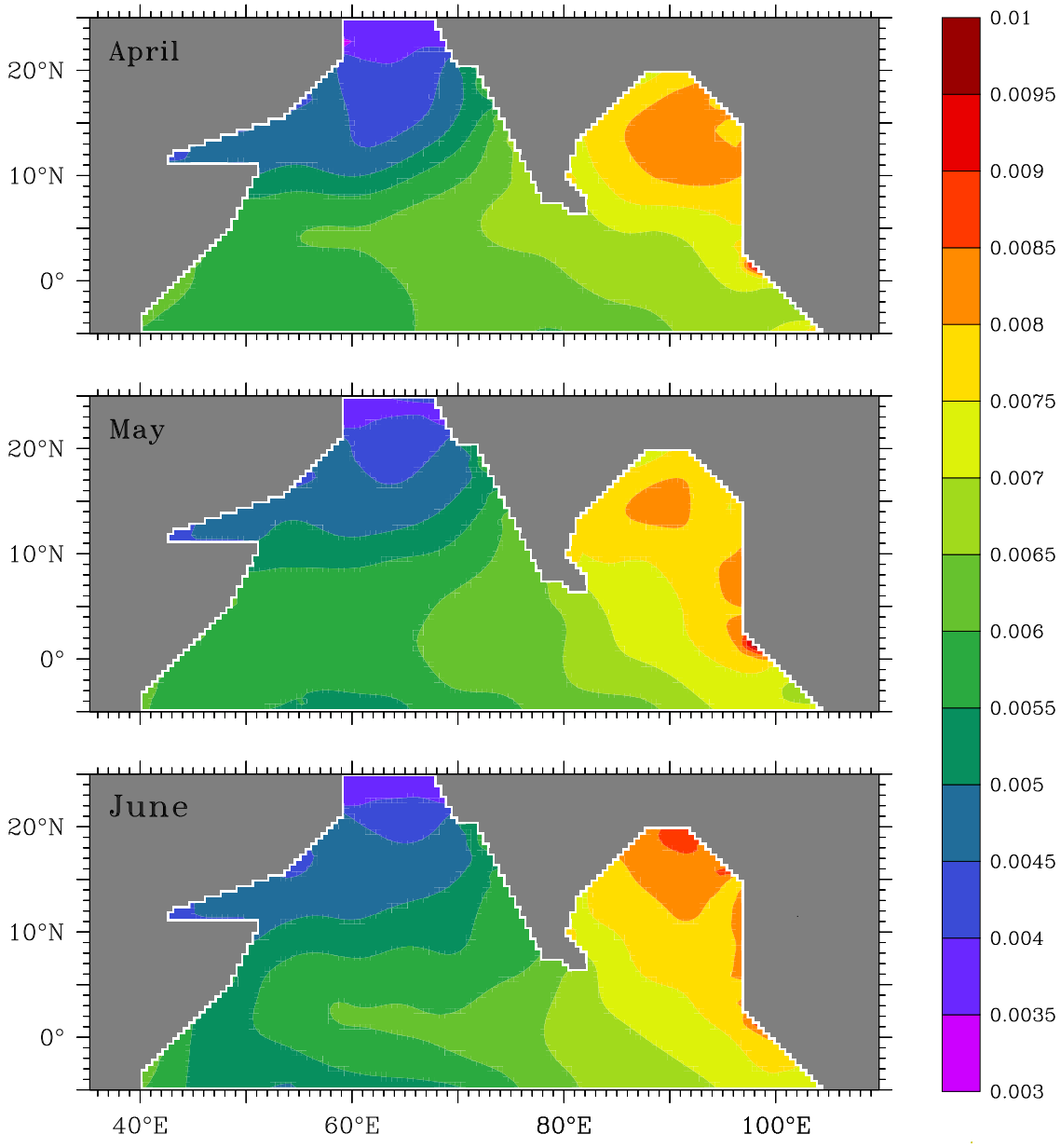

Figure 4.8 (continued) The seasonal cycle of the reduced-gravity parameter Γ in the north Indian Ocean. Γ is computed from the monthly climatologies of Levitus and Boyer [1994] and Levitus et al. [1994]. The southwest monsoon brings about a large change in Γ, especially in the Bay of Bengal. The largest increase (decrease) in Γ (density) is along the east coast of India, and along the west coast of Myanmar (Burma), which forms the eastern boundary of the northern bay. The tongue of low-salinity water (high Γ) in the equatorial Indian Ocean also stretches westward.

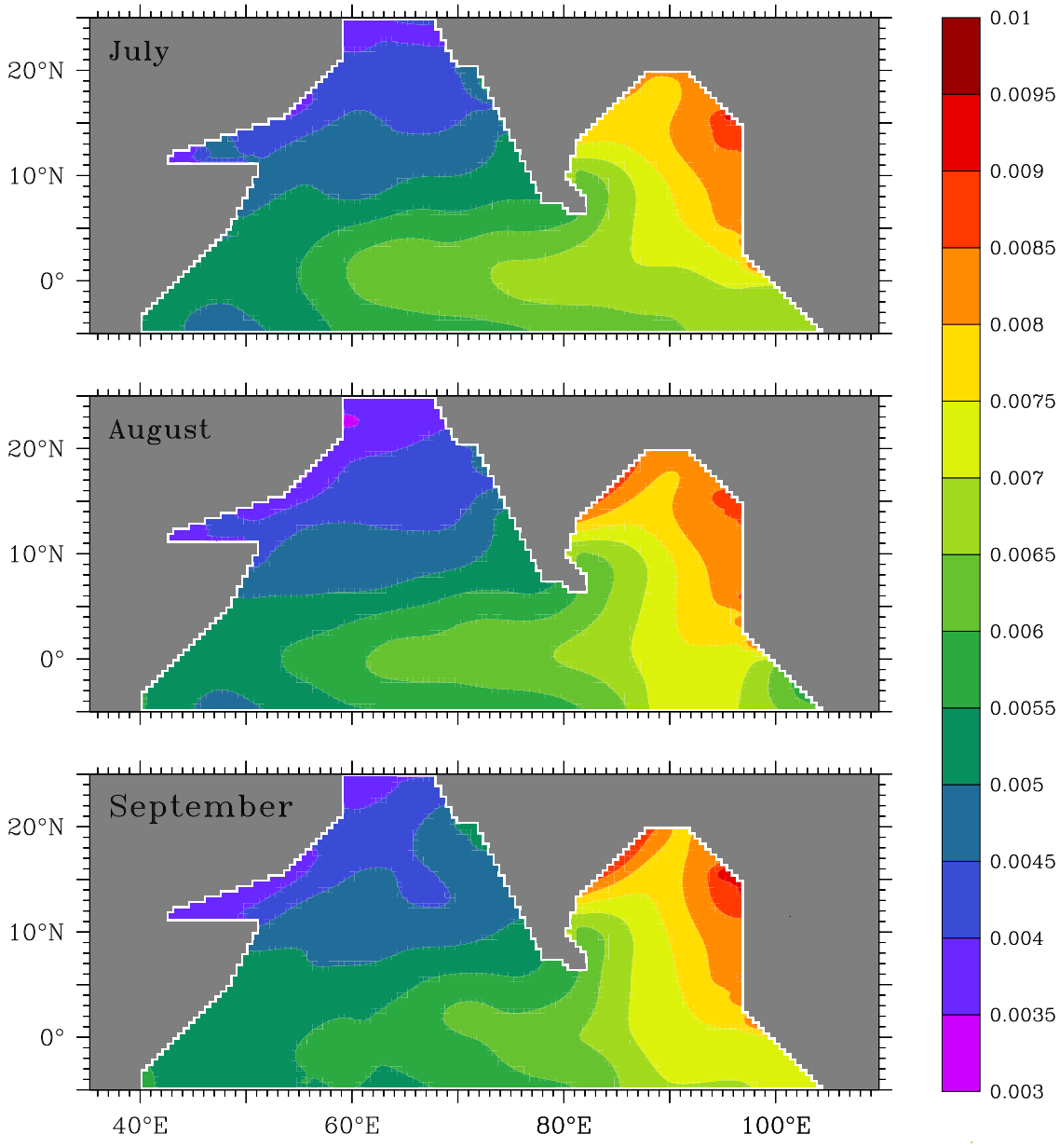

Figure 4.8 (continued) The seasonal cycle of the reduced-gravity parameter Γ in the north Indian Ocean. Γ is computed from the monthly climatologies of Levitus and Boyer [1994] and Levitus et al. [1994]. With the collapse of the southwest monsoon, salinity increases along the east coast of India and Sri Lanka in the monthly climatology of Levitus et al., leading to an increase in Γ. Γ, however, increases along the west coast of India, especially in the south, owing to an inflow of low-salinity water from the bay and the decrease in temperature due to the cessation of upwelling.

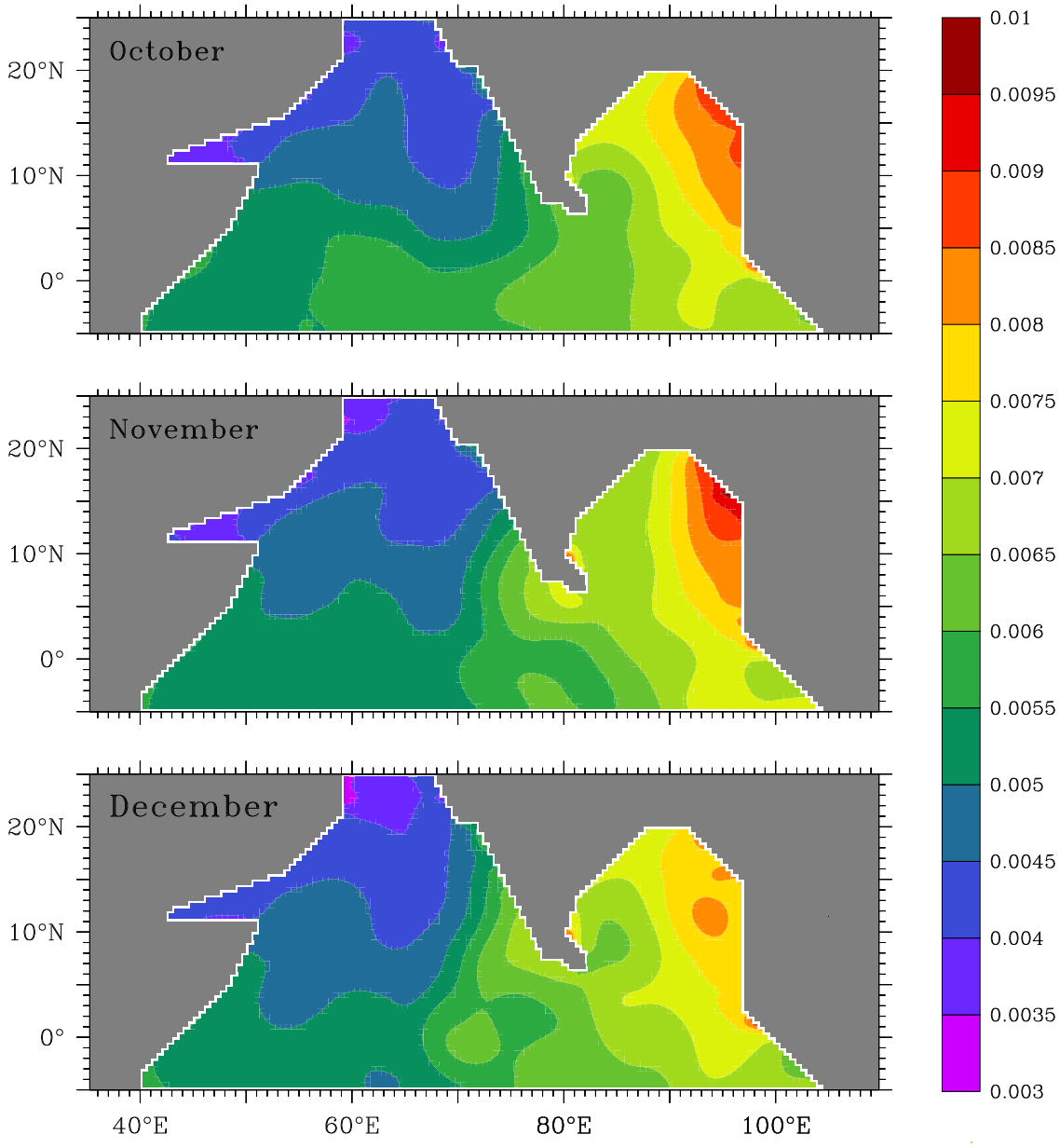

Figure 4.9 The seasonal cycle of Γ along the coast of India. The density of the upper layer is computed from the monthly climatologies of Levitus and Boyer [1994] and Levitus et al. [1994]. The figure shows Γ, Γ_T, and Γ_S; Γ_T and Γ_S are the contributions of temperature and salinity to Γ. Along the west coast, both temperature and salinity are important, the decrease in temperature because of upwelling associated with the Lakshadweep low causing a drop in Γ during the southwest monsoon. After the southwest monsoon, Γ increases because of the cessation of upwelling and an inflow of low-salinity water from the Bay of Bengal. Along the east coast, temperature is unimportant; it is salinity that controls the density in the upper layer. In the monthly climatology of Levitus et al., salinity is minimum, and hence, Γ is maximum, in September. Γ is minimum during November and December.

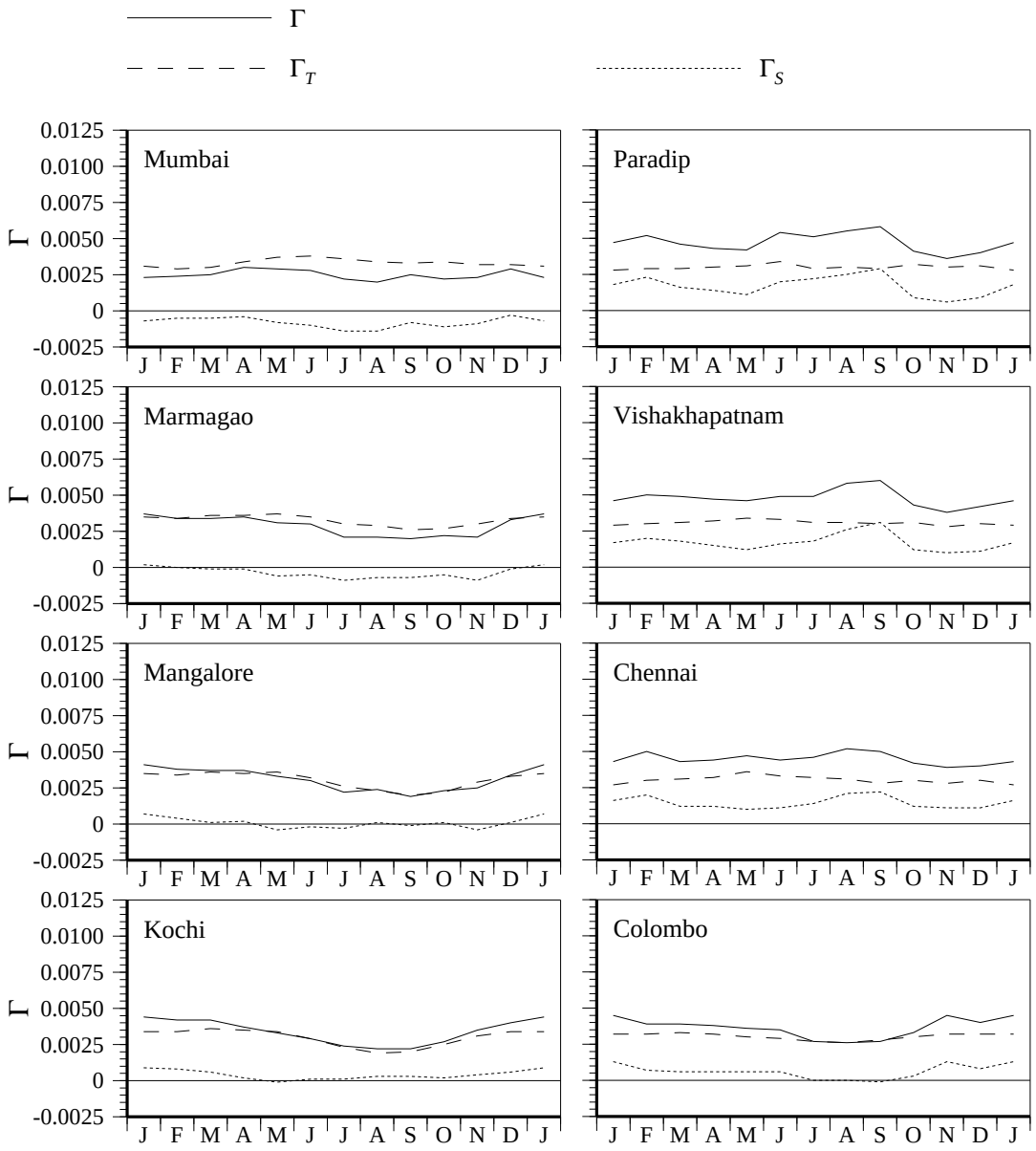

Figure 4.10 Effect of variable density on the seasonal cycle of surface circulation in the north Indian Ocean; apart from the density variation in the upper layer, the simulation is identical to the nonlinear simulation in Section 3.3.2 (Figure 3.5). Sea-level deviation η (cm) and velocity $\mathbf{v}$ (cm s^{-1}) are shown. The variations in density barely perturb the circulation, but there is a change in sea level; for example, sea level is higher in the anticyclonic high in the bay during February–May.

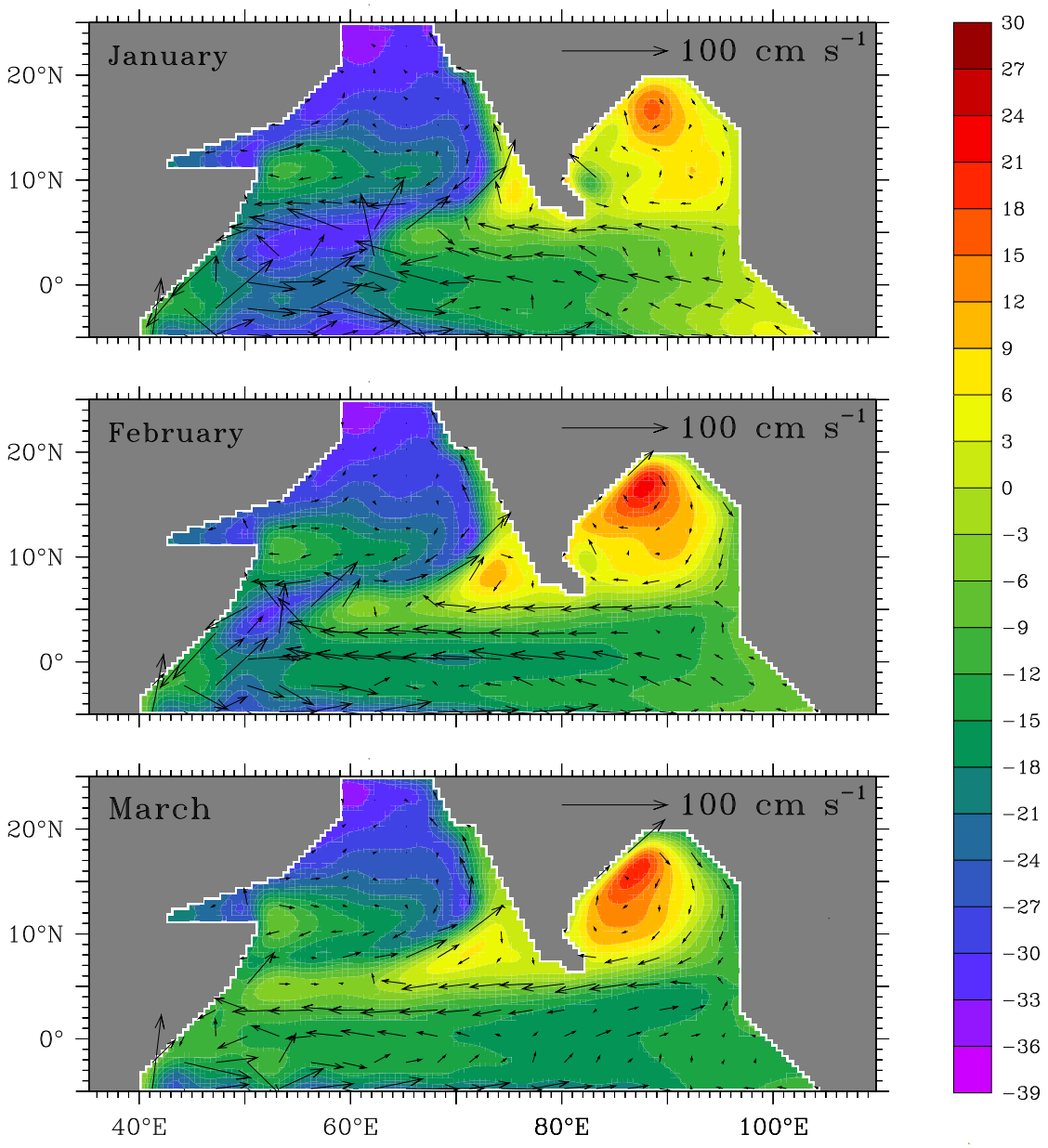

Figure 4.10 (continued) Effect of variable density on the seasonal cycle of surface circulation in the north Indian Ocean; apart from the density variation in the upper layer, the simulation is identical to the nonlinear simulation in Section 3.3.2 (Figure 3.5). Sea-level deviation η (cm) and velocity **v** (cm s^{-1}) are shown. Sea level rises in the northern bay and the eastern equatorial Indian Ocean, and it decreases in the northern and western Arabian Sea, the four regions most affected by the variations in density.

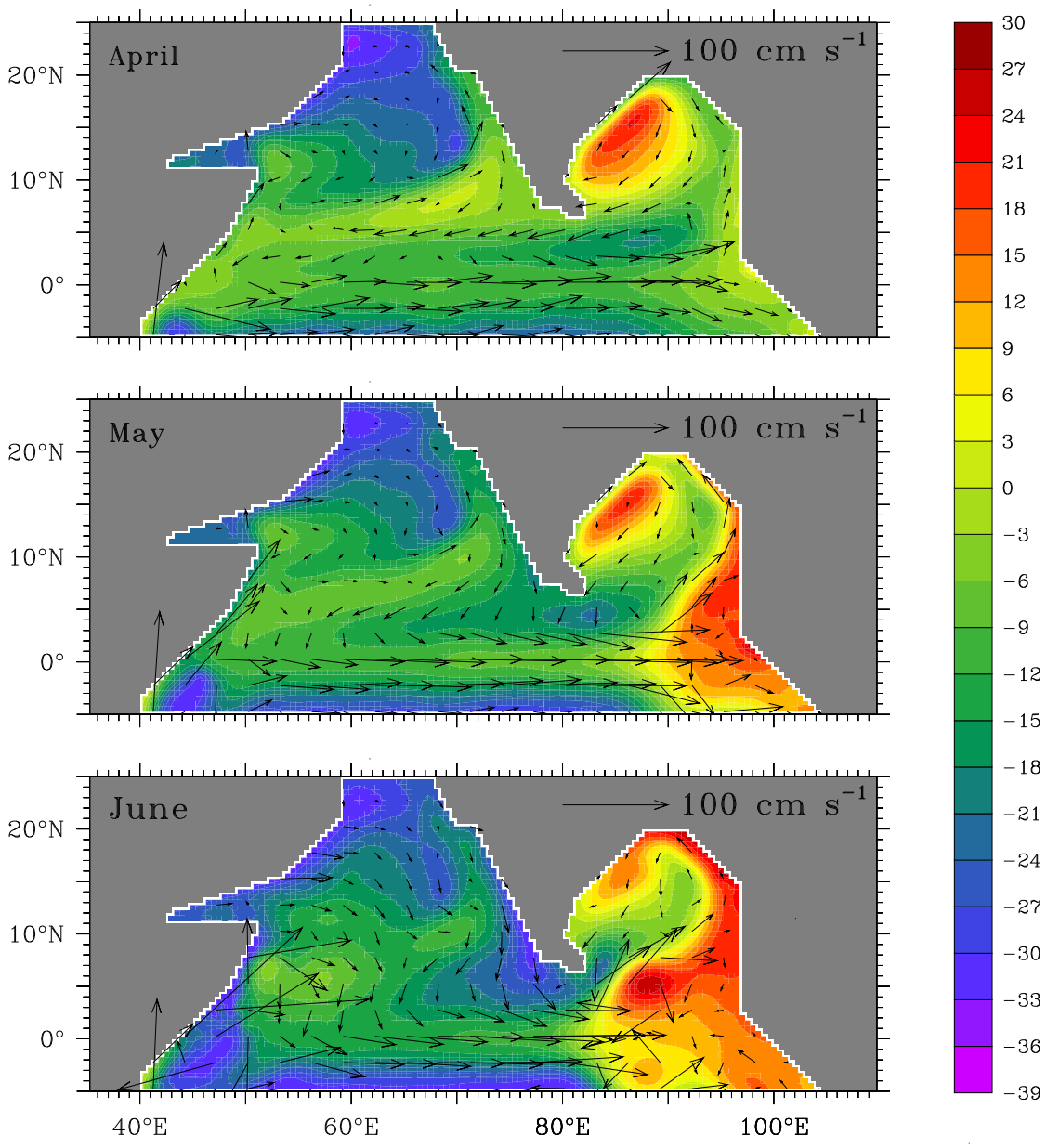

Figure 4.10 (continued) Effect of variable density on the seasonal cycle of surface circulation in the north Indian Ocean; apart from the density variation in the upper layer, the simulation is identical to the nonlinear simulation in Section 3.3.2 (Figure 3.5). Sea-level deviation η (cm) and velocity $\mathbf{v}$ (cm s^{-1}) are shown. The increase in density in the western Arabian Sea has an effect on the sea level and the circulation off the Somali coast; the Great Whirl is weaker than in the constant-density simulation. This is the only occasion when the variations in density have an impact on the circulation.

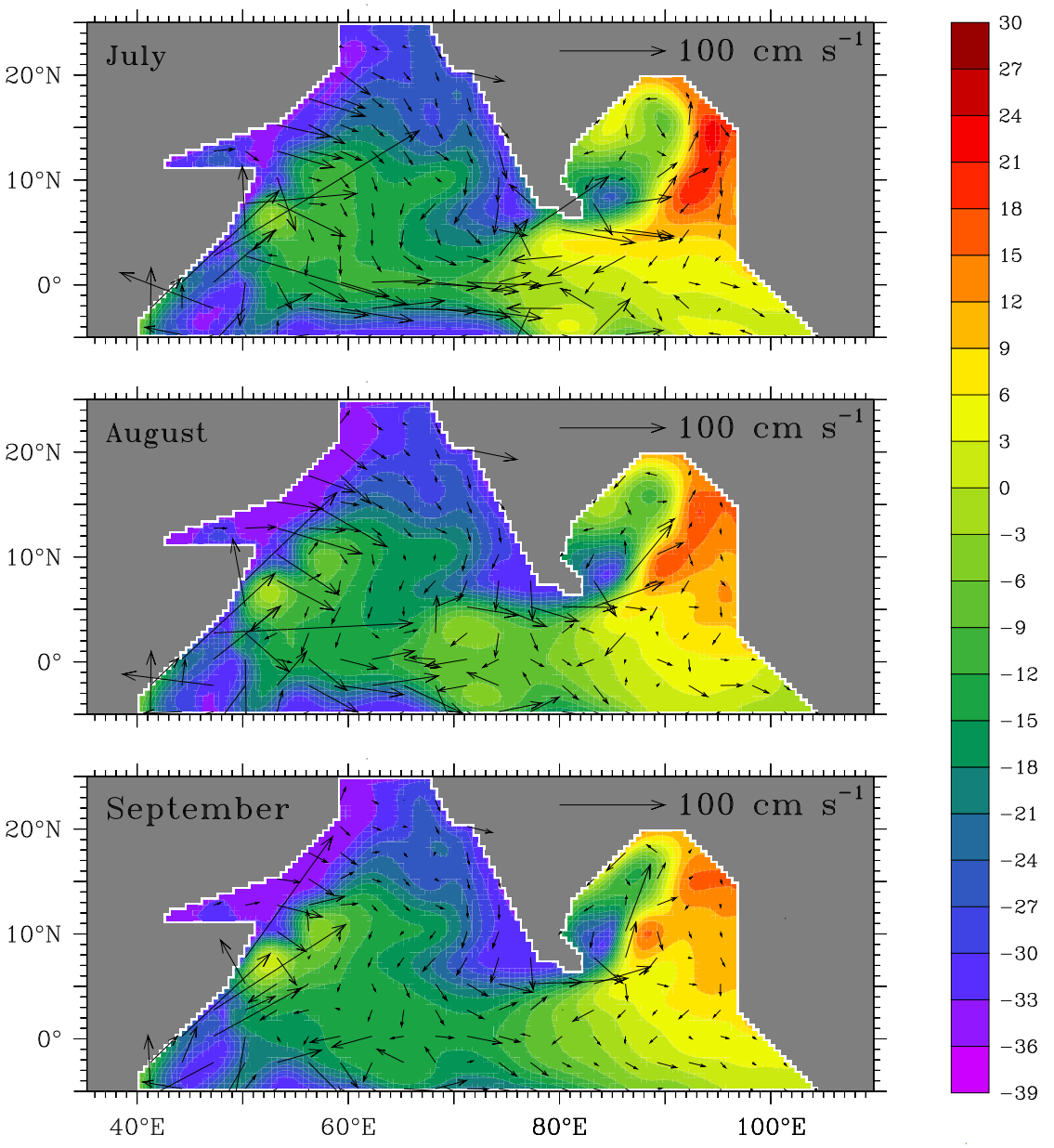

Figure 4.10 (continued) Effect of variable density on the seasonal cycle of surface circulation in the north Indian Ocean; apart from the density variation in the upper layer, the simulation is identical to the nonlinear simulation in Section 3.3.2 (Figure 3.5). Sea-level deviation η (cm) and velocity **v** (cm s^{-1}) are shown. The after-effects of the southwest monsoon persist in the western Arabian Sea till December; the sea level there is lower than in the constant-density simulation and the currents are a little weaker.

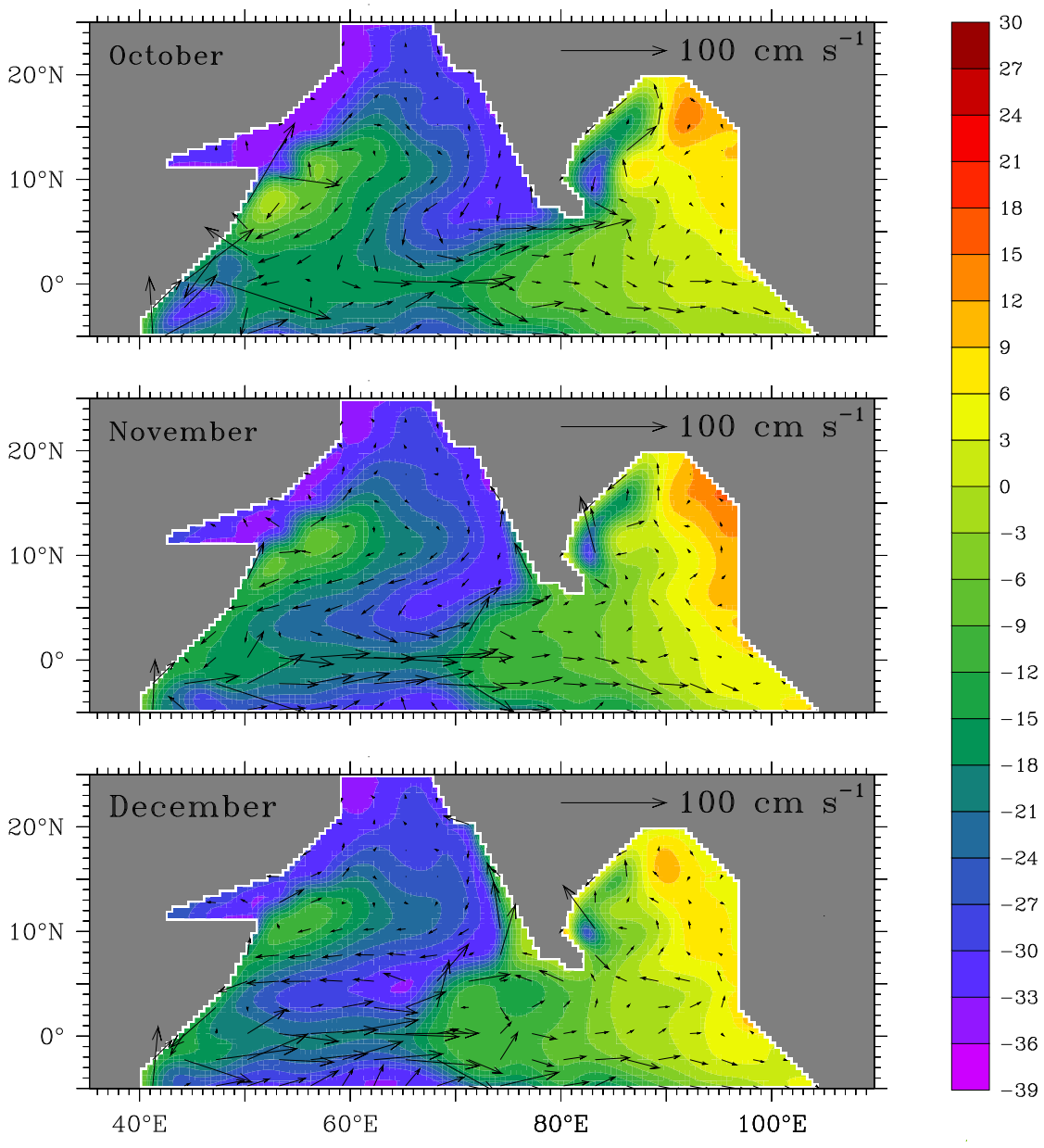

Figure 4.11 Effect of salinity on the seasonal cycle of model alongshore currents. Alongshore ship drifts (cm s^{-1}), from the climatology of Rao et al. [1989], are plotted along with the alongshore currents (cm s^{-1}) from the simulations with constant upper layer density and with variable upper layer density in a $1\frac{1}{2}$-layer reduced-gravity model. The density of the upper layer in the variable-density model is computed from the monthly climatologies of Levitus and Boyer [1994] and Levitus et al. [1994]. All variables plotted are anomalies; the annual mean has been removed. The variations in density force minor changes in the current along the coast of India; the increase in velocity, however, necessitates a change in the scale of the ordinate (see Figure 4.2).

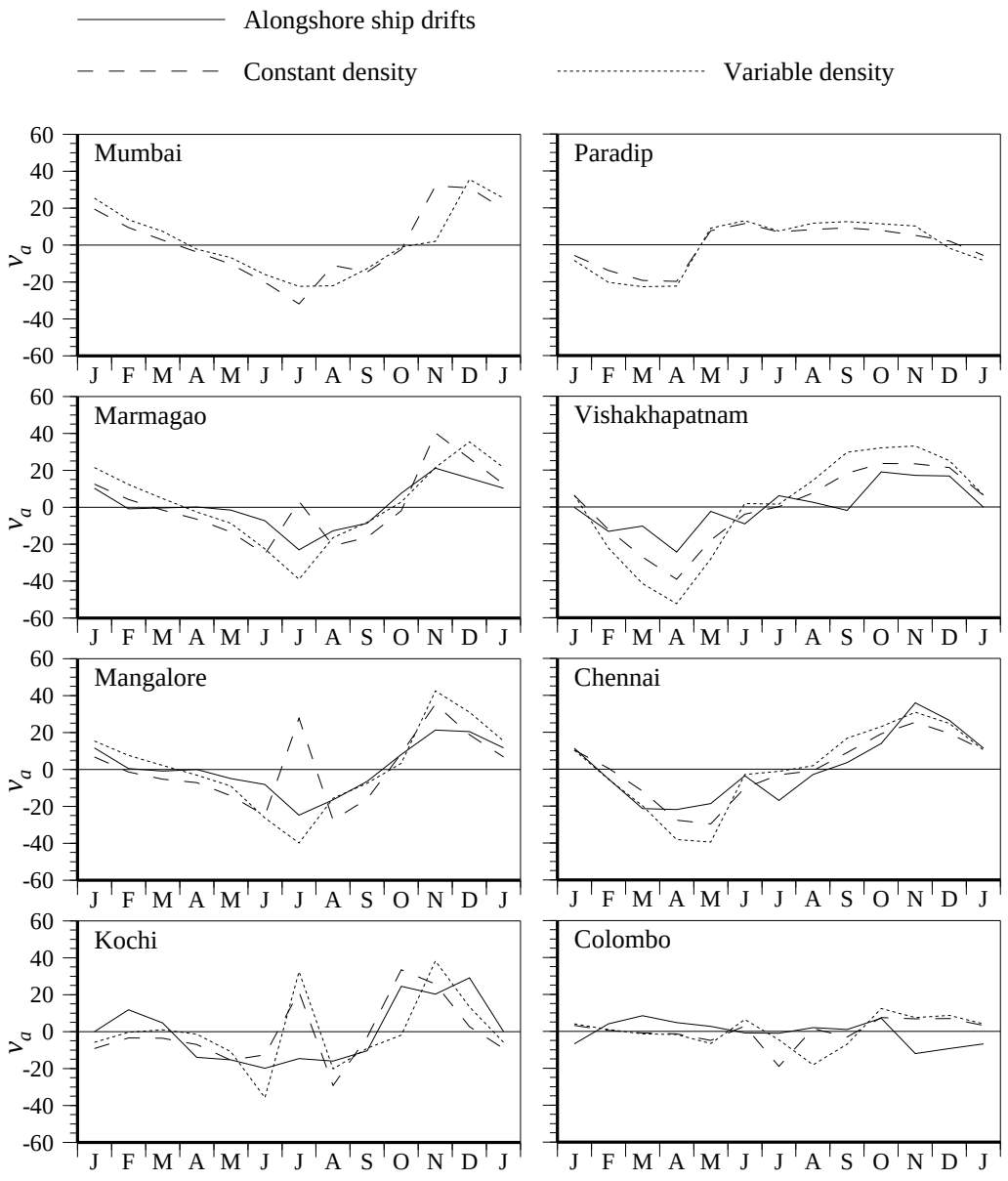

Figure 4.12 Effect of salinity on the seasonal cycle of sea level. Monthly anomalies of corrected sea level (cm) are plotted along with those from the simulations with constant and variable upper layer density in a $1\frac{1}{2}$-layer reduced-gravity model. The increase in Γ along the east coast has an effect on sea level only at Paradip in the northern bay, where the density changes are significant, but this increase is restricted to the southwest monsoon. The effect of a decrease in salinity during September is offset by upwelling forced by the EICC. During November, when the EICC favours downwelling, salinity increases in the monthly climatology of Levitus et al.. Therefore, the model still fails to simulate the maximum along the east coast.

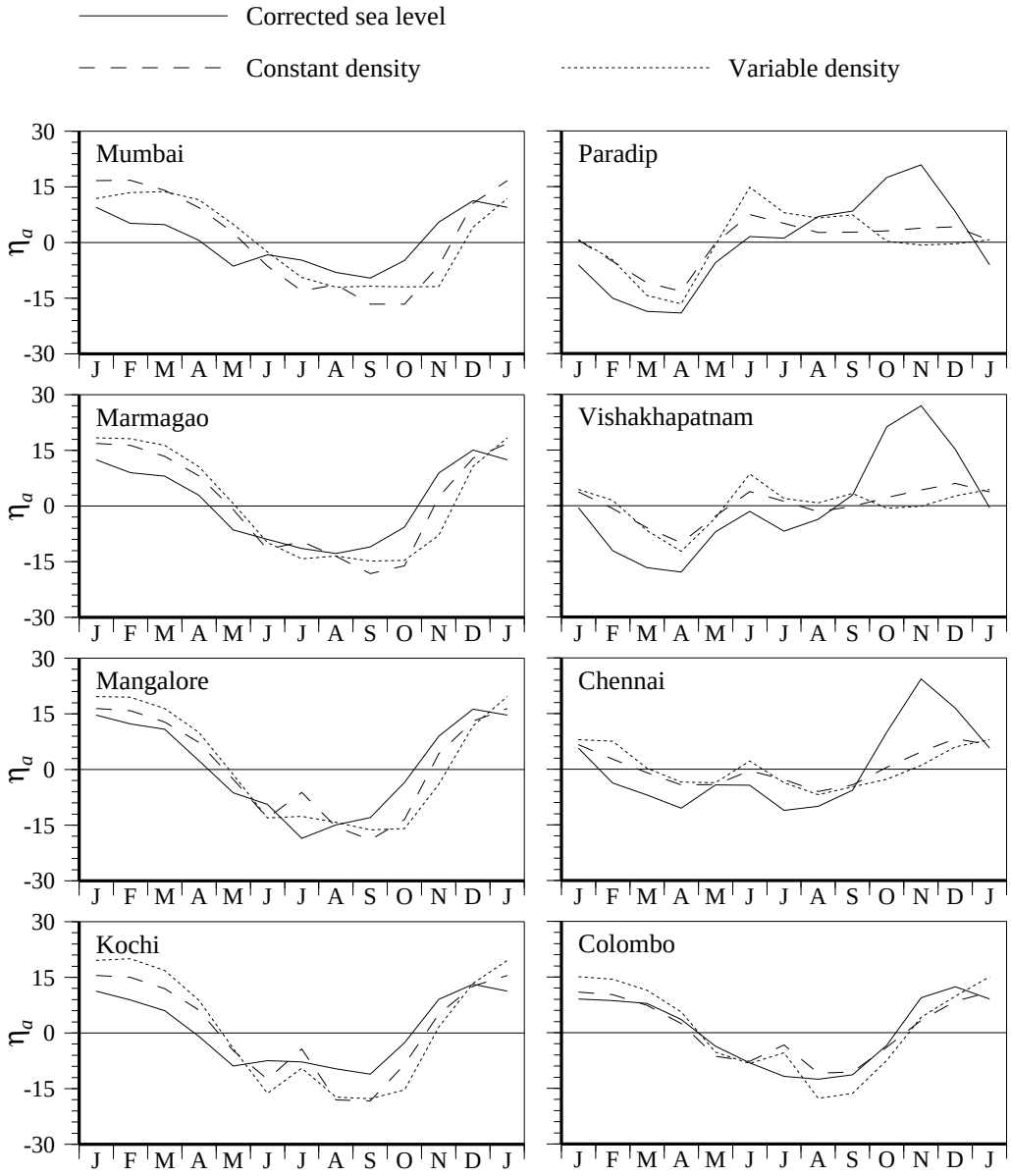

data in the coastal waters of India[5] [Rao, 1998]; this is especially true of salinity. The absence of data in the coastal waters of India makes it necessary to extrapolate from the data in the open bay, which too are sparse. Hence, the monthly climatologies of Levitus and Boyer and Levitus et al. are not reliable in the vicinity of the coast; a comparison with the hydrographic data collected during the six EEZ cruises (Section 2.4) [Shetye et al., 1990, 1991a,b, 1993, 1996] shows that the climatology of Levitus et al. does not capture the seasonal cycle of salinity correctly.

4.3.2 Monsoon Rainfall and the Seasonal Cycle of Salinity

There is considerable spatial and temporal variation in rainfall over the Indian subcontinent and the surrounding ocean, and this leads to the large differences in salinity along the coast. The Indian west coast receives very high rainfall, about 200 cm year^{-1}, almost 90% of which is during the southwest monsoon (June–September). The high rainfall is because of the Sahyadri range (or Western Ghats) running parallel to the coast about 100 km inland (Figure 4.13); this range blocks the moisture-rich monsoon winds. The resulting runoff is carried to the Arabian Sea by numerous swift, seasonal streams. Over the rest of the subcontinent, there is considerable spatial variability in the amount of rainfall, but about 80% is received during the southwest monsoon. Most of this rain falls in the catchment areas of eastward-flowing rivers (Figure 4.13), whose inflow into the Bay of Bengal peaks in August, a month after the peak in rainfall. About 70% of this inflow comes from the Ganga and the Brahmaputra, which discharge about 7.2×10^{11} m^3, the fourth largest discharge in the world, into the northern bay during June–October [Martin et al., 1981; Shetye, 1993]. Therefore, the quantum of freshwater inflow from the rivers into the seas around India is highly seasonal.

Equally seasonal are the coastal currents around India[6]. The weakening of the southwest monsoon winds after July, coupled with remote forcing from the eastern Bay of Bengal and the equatorial Indian ocean, forces an equatorward EICC in the northern bay; the EICC is poleward along the rest of the Indian east coast. Together, these currents trap the runoff in the northern bay. As the southwest monsoon withdraws and the northeast monsoon sets in, the equatorward EICC expands southward, forcing coastal downwelling and advecting the riverine inflow as a coastally-trapped low-salinity plume that is nearly 60 m deep [Shetye et al., 1996]. By November, the EICC is equatorward all along the east coast and there is a sharp drop in the salinity along the coast. The EICC flows into the westward NMC, which bends around Sri Lanka and flows along the western flank of the Lakshadweep high into the poleward WICC; the riverine inflow into the Bay of Bengal is thus transported into the Arabian Sea. This inflow is spread along the west coast

[5]This is due to the restrictions put by India on the use of data, hydrographic or otherwise, collected in the Indian Exclusive Economic Zone (EEZ).

[6]See Chapters 2 and 3.

Figure 4.13 The major rivers of India; the dashed line shows the 200 m isobath. Most of the big rivers flow eastward into the Bay of Bengal. The highest runoff is that of the Ganga and Brahmaputra, which together empty about 7.2×10^{11} m^3 into the northern bay during June–October. Most of these rivers originate either in the Himalayas or in the Sahyadri range (Western Ghats), which is about 1 km high and runs parallel to the west coast of India. Smaller, swift streams flow westward from the Sahyadris into the Arabian Sea, and their combined runoff is about 30% that of the Ganga and the Brahmaputra. This runoff is assumed to be 80% of the total rainfall in the coastal belt that stretches from the southern tip of India to just north of Mumbai and is bounded in the east by the Sahyadri range. The abbreviations used in the figure are as follows: EICC, East India Coastal Current; WICC, West India Coastal Current; NMC, Northeast Monsoon Current; LH, Lakshadweep high; R.G., River Ganga; R.B., River Brahmaputra. The currents are plotted for December, when the EICC flows equatorward and the WICC flows poleward. Together, they transport low-salinity water from the northern bay to the west coast of India.

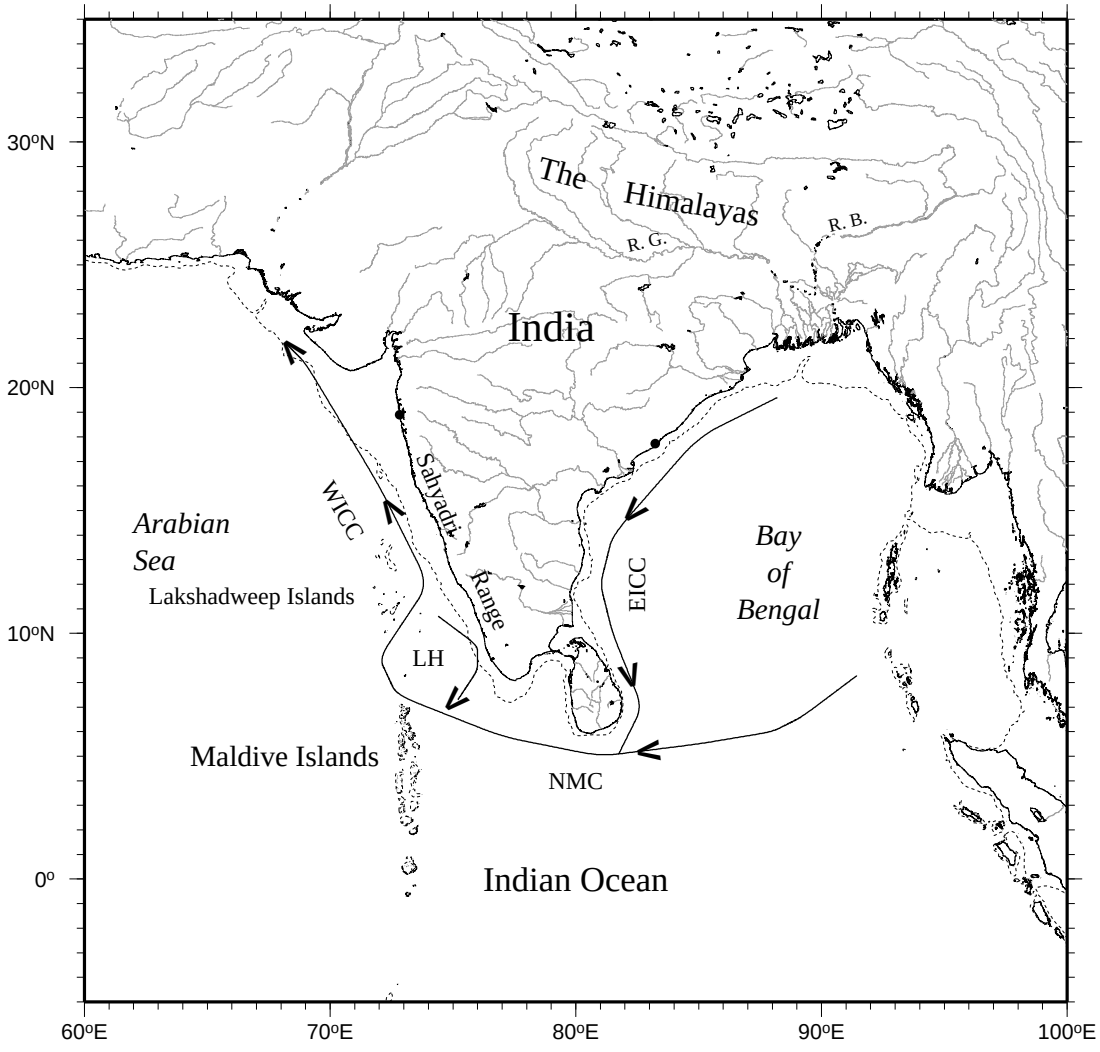

of India by the WICC and is spread offshore in the southern part of the coast by the westward propagating Rossby waves that constitute the Lakshadweep high. By February, the EICC reverses to flow poleward, forcing coastal upwelling and raising salinity along the east coast [Shetye et al., 1993]. The WICC along the northern part of the west coast, however, continues to flow poleward till March, spreading the low-salinity water from the bay, as well as the inflow from local rivers during the southwest monsoon, along the west coast.

During the southwest monsoon, when the freshwater actually enters the Indian coastal regime, the EICC and WICC favour upwelling, and hence, the low-salinity water is trapped at the surface and pushed offshore by the Ekman flow, except in the northern bay, where the remotely-forced equatorward EICC traps the river runoff. It is only after the southwest monsoon, when these currents reverse, that the low-salinity water is pushed towards, and advected along, the coast. Even along the west coast, the lowest salinities at the surface are during the southwest monsoon, but the drop in salinity is restricted to a shallow surface layer. As along the east coast, it is during the northeast monsoon, when the WICC favours downwelling and there is inflow of freshwater from the Bay of Bengal, that the low-salinity layer deepens, this being more pronounced off southwest India where the low-salinity water spreads offshore because of the Lakshadweep high.

The seasonal cycle of salinity along the coast of India is shown in Figures 4.14 and 4.15, which are based on the six EEZ cruises. These data represent but a snapshot and were collected over a few years. Interannual variability is expected to cause changes in these fields, but they nevertheless provide a rough picture of the seasonal cycle of salinity in the coastal waters of India. Unlike in the data of Levitus et al. [1994], salinity, averaged over the top 100 m, is lowest along the east coast *after* the southwest monsoon. The error in the monthly climatology of Levitus et al. is owing to the linear interpolation from their seasonal climatology and the lack of data in the coastal waters of India. Therefore, to examine the effect of salinity on the seasonal cycle of sea level along the east coast of India, we synthesize a seasonal cycle of the coastal salinity field from the available data. We cannot, however, use the data from these six cruises and interpolate to synthesize the seasonal cycle because of the rapid changes in the coastal currents off India and the associated rapid changes in the coastal salinity and temperature fields due to upwelling and downwelling. A better approach is to use all the available salinity data in the vicinity of the coast to construct a climatology of coastal salinity, which can be used in conjunction with the salinity climatology of Levitus et al. [1994] in the simulations.

4.3.3 Synthesis of a Climatology of Temperature and Salinity Along the Coast

To construct the “coastal climatology”, we use hydrographic data available at the Indian National Oceanographic Data Centre (INODC). These data were collected over several cruises, the earlier

Figure 4.14 Seasonal cycle of surface salinity (PSU) in the coastal waters of India, based on the six EEZ cruises. The "+" indicate the locations at which the hydrographic profiles were obtained. The time of the cruises are mentioned in addition to the months they are considered representative of. The minimum and maximum salinity and the contour interval (CI) are listed for each cruise.

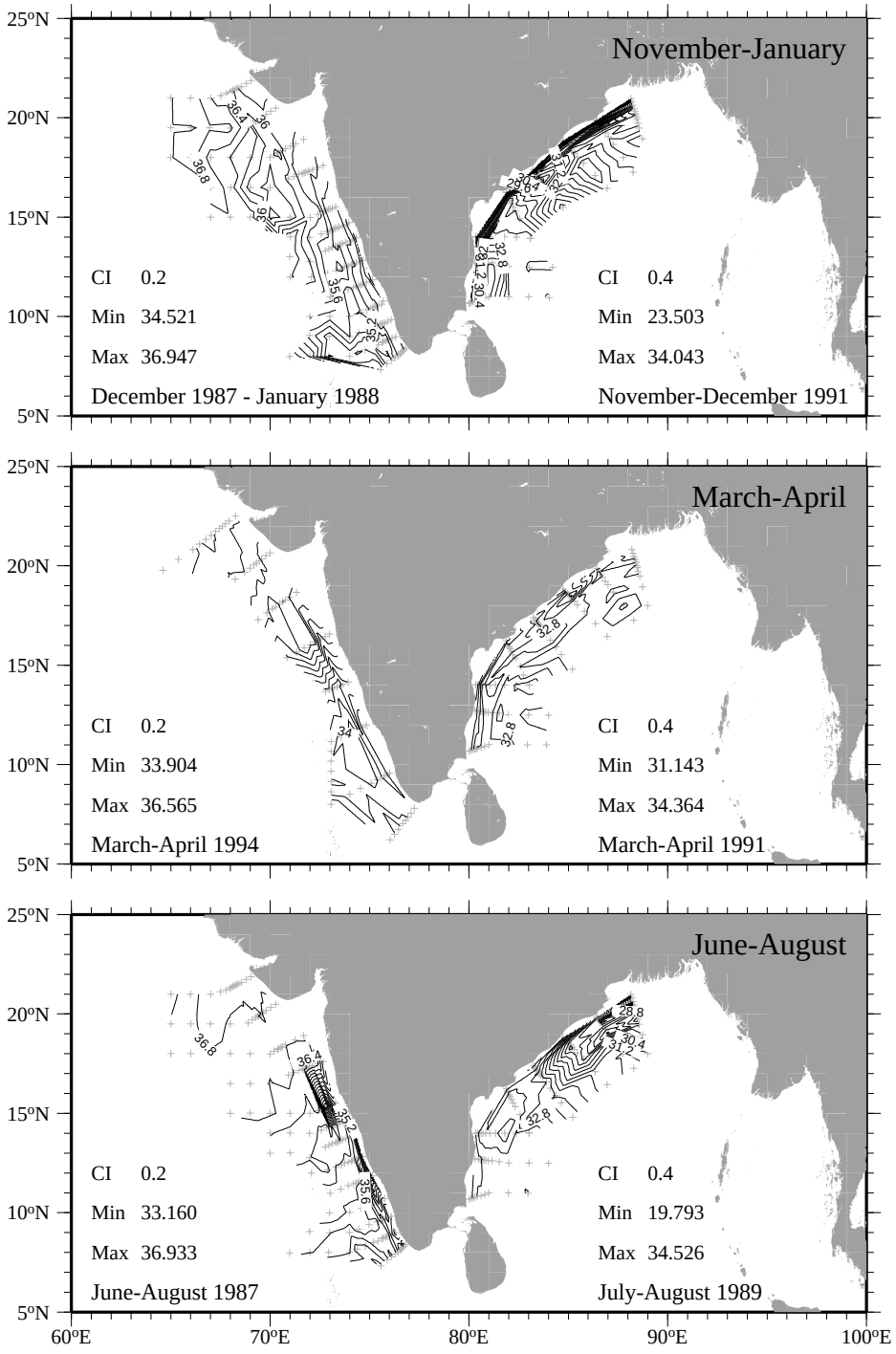

Figure 4.15 Vertical cross-sections of salinity (PSU) off Vishakhapatnam (right) and Marmagao (left). The distance from the coast (km) is plotted on the abscissa and depth (m) on the ordinate. The cross-sections are based on the six EEZ cruises.

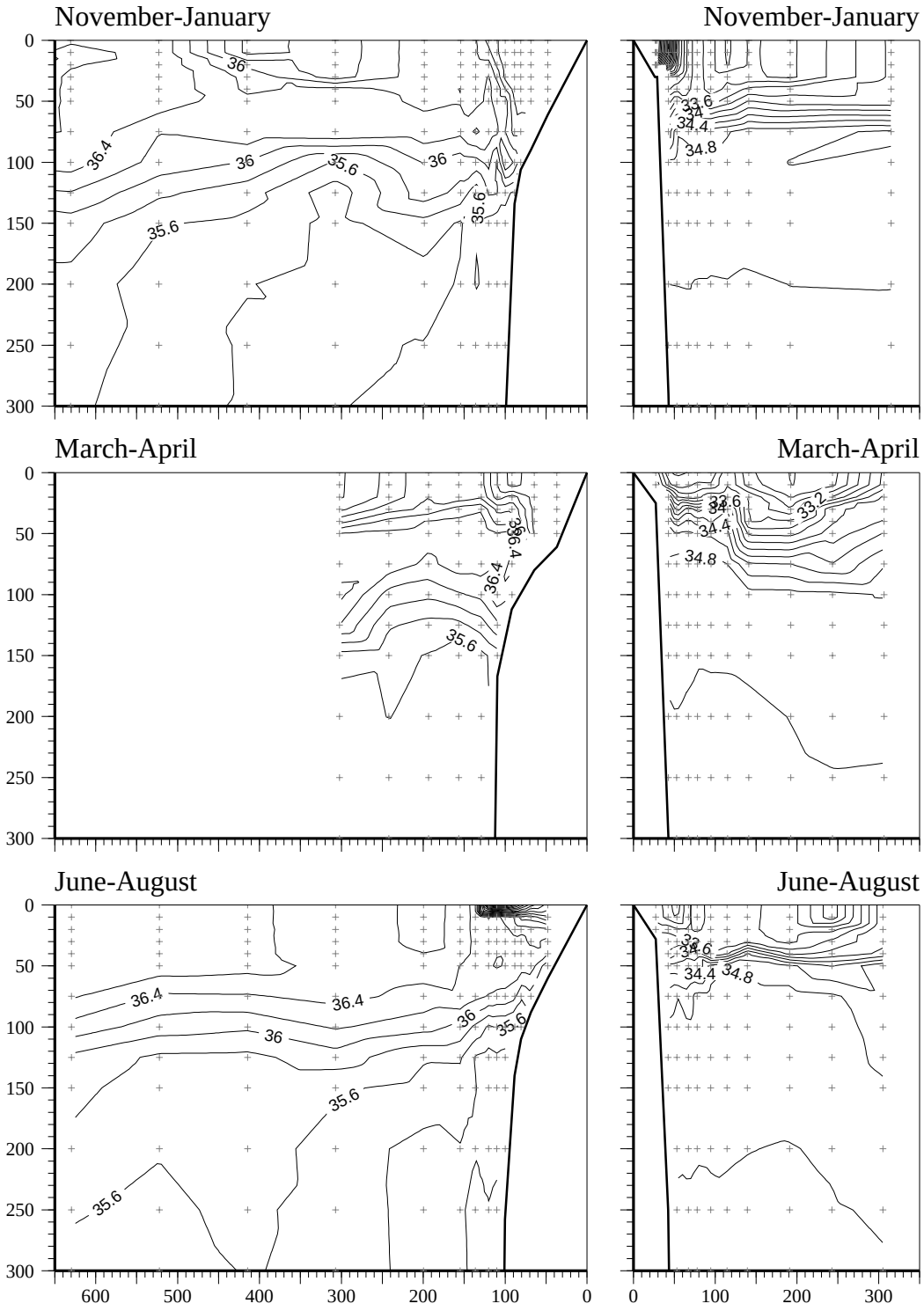

cruises using Nansen bottles and the later cruises using CTDs[7] to obtain a vertical profile of temperature and salinity. The data are available at the standard depths[8]. We bin the data in a $1^\circ \times 1^\circ$ box around Paradip, Vishakhapatnam, Chennai, Kochi, Mangalore, Marmagao, and Mumbai to construct a climatology for these boxes, and then use linear interpolation to obtain a continuous distribution of temperature and salinity along the coast, this process being being repeated for each month[9]. This method works well and yields a better synthesis than is possible using just the six EEZ cruises. The only caveat is that data are not available for some months at some of these seven stations, the data at Paradip having the maximum number of gaps. Given the description of the seasonal cycle of the currents and the available data, it is possible to interpolate to fill these gaps. The difficult month, however, is November, for which no salinity data are available along the east coast! The deep low-salinity plume along the east coast was surveyed in December by Shetye et al. [1996]; hence, the lowest salinity reported along the east coast is for that month. Linear interpolation is ruled out, given the rapid changes in salinity that take place after the collapse of the southwest monsoon. To get over this problem, we use the values for December as a guide, and assume that the salinity in November is *lower* than in December. There are two reasons for making this assumption. First, the equatorward EICC manifests along the coast after the collapse of the southwest monsoon, appearing first in the northern bay. The Kelvin wave that forces it propagates equatorward along the coast and the EICC reverses all along the east coast in October. Since the current speed is of the order of 25 km day^{-1} [Shetye et al., 1996], it would take about a month to transport the low-salinity water down the coast to Chennai; hence, we expect the salinity to be lowest in late October or in early November. Second, the equatorward EICC is strongest in November; it weakens in December and begins reversing in January, forcing coastal upwelling and raising salinity all along the east coast; hence, we expect the salinity to be lower in November than in December.

We choose salinities sufficiently low to produce the sharp peak in sea level observed in November. Then, if these values are not unreasonable, we would have a hypothesis to explain the seasonal cycle of sea level along the coast of India. The synthesized seasonal cycles of temperature and salinity, averaged over the top 100 m of the water column, are shown in Figures 4.16 and 4.17 for the stations along the coast; the seasonal cycle of the resulting reduced-gravity parameter Γ is shown in Figure 4.18.

[7] Conductivity-Temperature-Depth.

[8] The standard depths (m) are 0, 10, 20, 30, 50, 75, 100, 125, 150, 200, 250, 300, 400, 500, 600, 700, 800, 900, 1000, 1100, 1200, 1300, 1400, 1500, 1750, 2000, 2500, 3000, 3500, 4000, 4500, 5000, and 5500.

[9] We interpolate linearly between the climatologies of Levitus and Boyer [1994] and Levitus et al. [1994] at the northeastern corner of the Bay of Bengal and the "new" climatology at Paradip, and between the "new" climatology at Mumbai and the climatologies of Levitus and Boyer and Levitus et al. at Veraval (see Figure 2.1) to obtain a smooth transition along the coast. There still remains a sharp density jump offshore, but this is not of major consequence for our problem.

Figure 4.16 The seasonal cycle of temperature (°C), averaged over the top 100 m of the water column, along the coast. The synthesized seasonal cycle is plotted along with that from the climatology of Levitus and Boyer [1994]. The method used to synthesize the climatological seasonal cycle is described in Section 4.3.3. The synthesized climatology of temperature is similar to that of Levitus and Boyer; the maximum difference in temperature is less than 2°C.

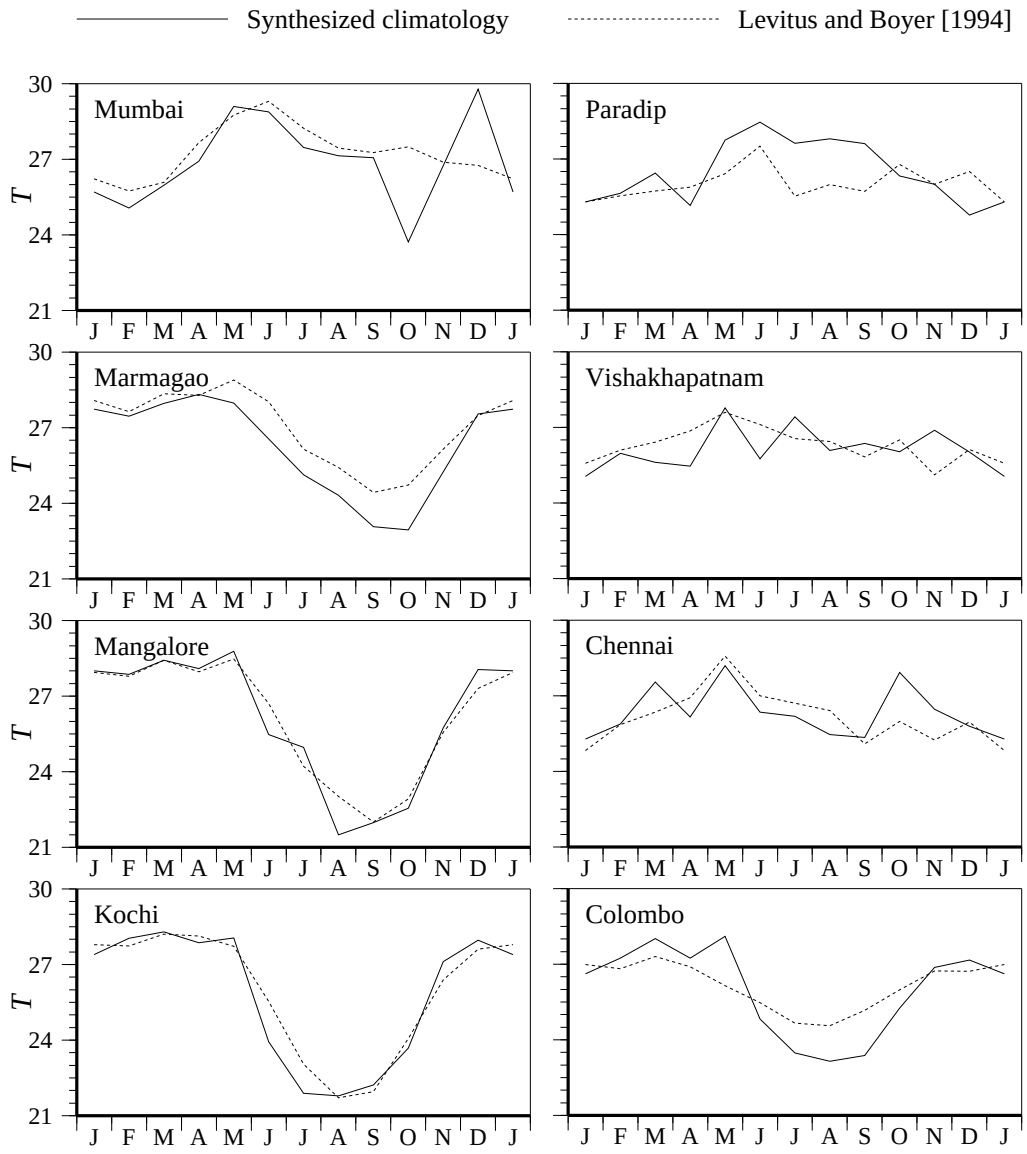

Figure 4.17 The seasonal cycle of salinity (PSU), averaged over the top 100 m, along the coast. The synthesized seasonal cycle is plotted along with that from the climatology of Levitus et al. [1994]. The method used to synthesize the climatological seasonal cycle is described in Section 4.3.3. The synthesized salinity matches that of Levitus et al., except along the east coast after the southwest monsoon. The inflow of freshwater during the southwest monsoon and its advection along the coast by the equatorward EICC after September result in a sharp drop in salinity along the coast.

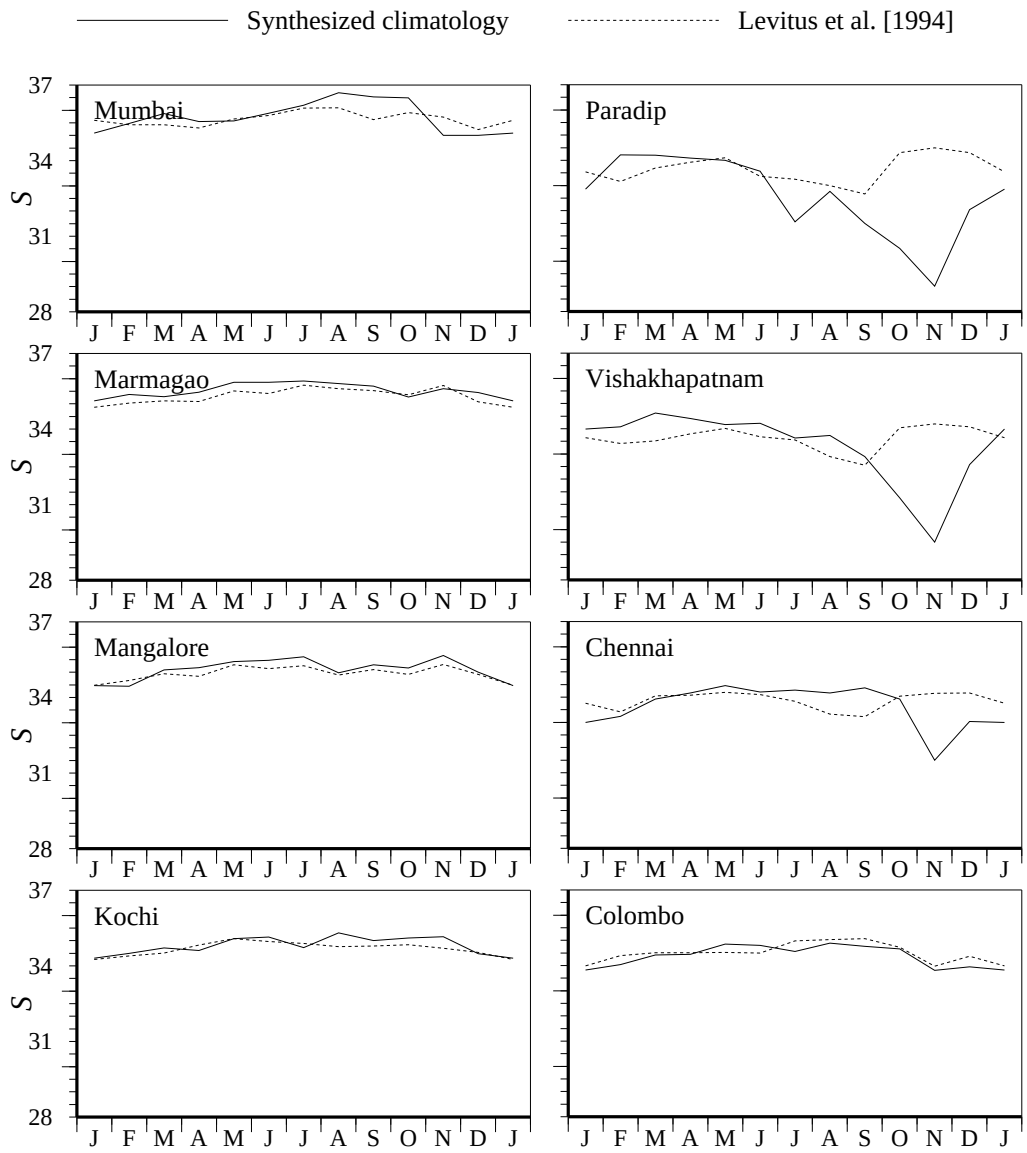

Figure 4.18 The seasonal cycle of Γ along the coast of India. The density of the upper layer is computed from the synthesized monthly climatology of temperature and salinity; the method of synthesis is described in Section 4.3.3. The figure shows Γ, Γ_T, and Γ_S; Γ_T and Γ_S are the contributions of temperature and salinity to Γ. Γ increases rapidly along the east coast after the southwest monsoon as the salinity and density decrease. The major contribution to Γ is from variations in salinity.

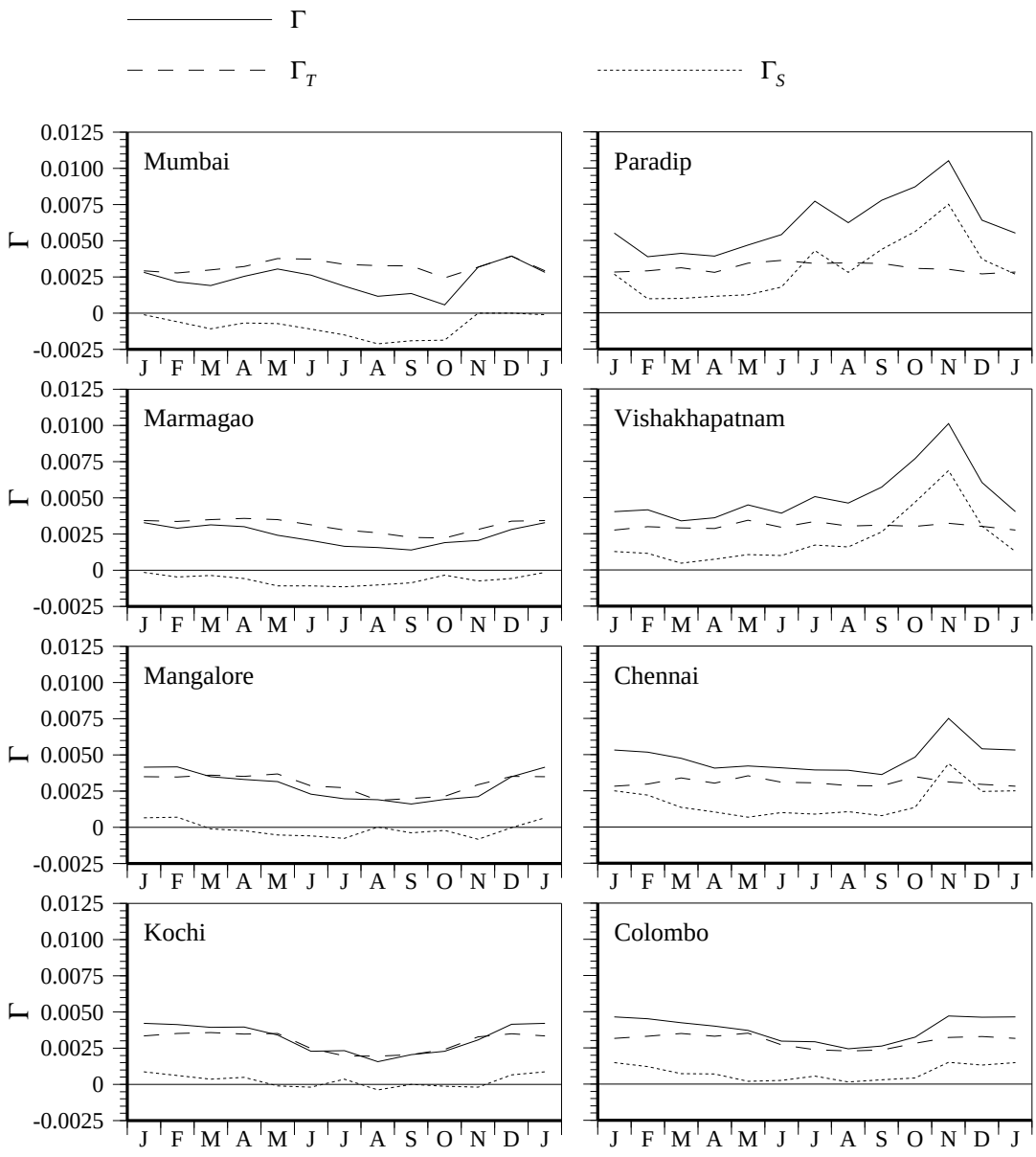

Figure 4.19 Effect of the synthesized salinity on the seasonal cycle of sea level. Monthly anomalies of corrected sea level (cm) are plotted along with those of sea level (cm) from the simulations with constant and variable upper layer density in a $1\frac{1}{2}$-layer reduced-gravity model. The density of the upper layer is computed from the monthly climatologies of Levitus and Boyer [1994] and Levitus et al. [1994], except along the coast of India, where the modified climatology is used. The lower salinity along the east coast in the synthesized climatology enables the model to simulate the sea level maximum in November; the seasonal cycle of model sea level now resembles that of corrected sea level.

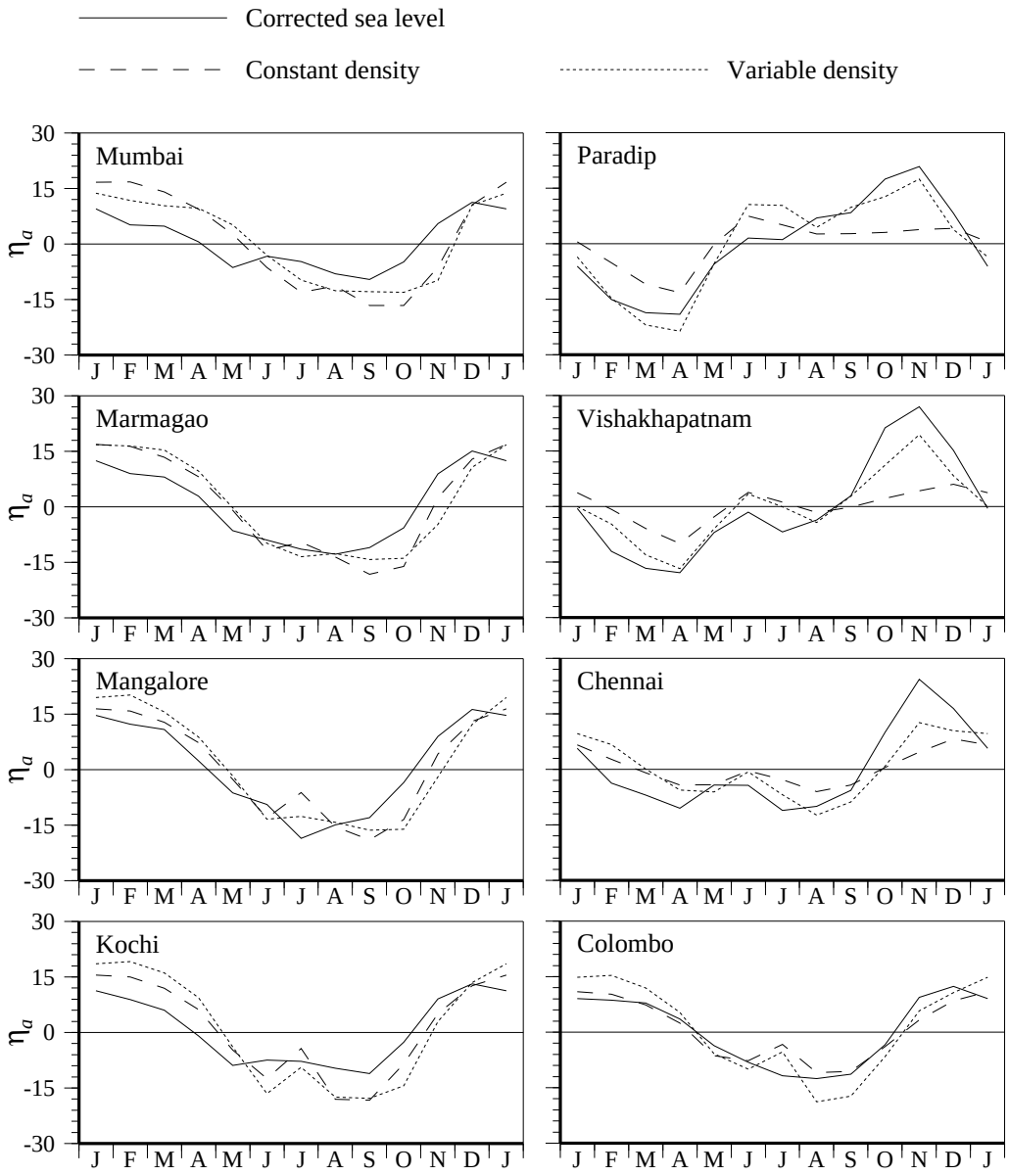

4.3.4 Simulations With the Synthesized Climatology

The synthesized climatology yields alongshore temperature and salinity fields from the northeastern corner of the Bay of Bengal to Veraval on the west coast of India. These are used to replace the coastal temperature and salinity data in the climatologies of Levitus and Boyer [1994] and Levitus et al. [1994], and this new climatology is used to determine Γ for the $1\frac{1}{2}$-layer model. The resulting sea level is shown in Figure 4.19. The synthesized coastal salinity improves the model's ability to simulate the seasonal cycle of sea level along the east coast. The changes made to the coastal salinity field have almost no impact on the west coast, but they raise sea level in November along the east coast, the seasonal cycle of model sea level now being similar to that of corrected sea level. The model sea level is still somewhat lower, implying that the salinity, averaged over 100 m, may be even lower than that assumed. We do not, however, have any data to support or deny this possibility.

In the absence of salinity data along the coast, it is difficult to go farther than this. Our aim has been to diagnose the causes of the seasonal cycle of corrected sea level along the Indian coast, and the somewhat *ad hoc* modifications made to the coastal salinity are justified in this context. A more acceptable approach would be to try to model the salinity, given the rainfall and the river runoff. This, however, is a much more complex task, one that we leave to the future. The simulations, however, are sufficient to warrant the inference that both wind-forced coastal currents and variations in coastal salinity are significant causes of the seasonal cycle of corrected sea level along the coast of India, the decrease in salinity along the east coast in November being responsible for the peak in sea level there. This decrease in salinity is due to the advection of the river runoff along the coast by the EICC. Advection is a nonlinear process; linearization of advection demands the existence of a well-defined mean. Since the variability of the currents and salinity along the coast of India is at least as large as the mean, this process cannot be linearized, unlike the wind-forced model of Chapter 3. The variations in salinity and density, however, have a comparatively minor impact on the alongshore currents; this implies that linear models are sufficient to describe the seasonal cycle of large-scale coastal currents, but not that of sea level, especially along the east coast of India.

4.4 Effect of Bathymetry: The Continental Shelf

One aspect of the reduced-gravity model that needs some discussion is the neglect of the continental shelf. The model assumes that the ocean has a flat bottom and that the continental boundaries are vertical walls. This simplification filters out those continental shelf waves and coastally-trapped waves that depend on shelf-bathymetry for their existence, with coastal Kelvin waves replacing them. In the ocean, the coastal Kelvin waves forced by the large-scale wind field are

modified in the vicinity of a coast, taking the form of continental shelf waves on the shelf in the absence of stratification, and that of coastally-trapped waves in the presence of stratification [Gill and Clarke, 1974; Mysak, 1980]. The Kelvin wave propagates with the shelf-break as the boundary, the continental slope acting as the vertical wall for the Kelvin wave, which therefore has its maximum amplitude at the shelf-break, the amplitude decaying exponentially offshore. Gill and Clarke [1974] showed that the movement of the thermocline due to the large-scale circulation was correlated with the changes in sea level at the coast. Therefore, a simple, heuristic idea of the effect of the shelf is the following. If the upper layer thickness is less than the depth of the continental shelf at the shelf-break, which usually is assumed to coincide with the 200 m isobath, the amplitude of the wave decays inshore too with an *e*-folding length scale given by the internal Rossby radius of deformation, R_i. If, on the other hand, the upper layer thickness is greater than the depth of the continental shelf at the shelf-break, the amplitude of the wave decays inshore with an *e*-folding length scale given by the external Rossby radius of deformation, R_e. Since R_i is proportional to the speed of the first baroclinic mode and R_e to the speed of the barotropic mode, $R_i \ll R_e$, and the amplitude decays faster inshore when the depth of the upper layer is less than 200 m. This description may not be valid at higher frequencies, but is reasonable at the seasonal and lower frequencies of interest to us.

The above effect of the continental shelf may be modified under certain circumstances, two of which are of interest to us. First, the strength of the coupling between the Kelvin wave and the shelf wave is of $O(\lambda)$, where $\lambda = \frac{R_i}{L}$, L being the shelf width [Allen, 1975; Mysak, 1980]. Off Mumbai, where the shelf is wide, this implies that the coupling is weak, and therefore the circulation on the shelf may be independent of that offshore. This, however, is unlikely because the seasonal cycle of sea level at Mumbai is similar to that at other stations along the Indian west coast, implying a link between coastal sea level and the large-scale circulation. The increased friction on the wide shelf, however, will alter the momentum balance and a likely consequence is a drop in the sea level at the coast. This would account for the model sea level being higher than the corrected sea level at Mumbai. Second, if there is a strong cross-shore salinity (or temperature) gradient on the shelf, as along the coast of India after the southwest monsoon, the decay in the amplitude inshore will be arrested by the low salinities, and the amplitude may even increase towards the coast. At the low frequencies of interest, this modification will be geostrophic, forcing a coastal current in the same direction as the large-scale coastal current. This would account for the model sea level being lower than the corrected sea level along the east coast. This discussion on the possible effect of the continental shelf on coastal sea level, however, is heuristic, and needs to be confirmed by observations and detailed model studies.

In conclusion, the presence of the continental shelf is not of major consequence for the seasonal cycle of sea level along the coast of India. The causes of this cycle are atmospheric pressure,

the wind-forced coastal currents, and the large changes in salinity, especially along the east coast. The difference in salinity between the east and west coasts of India results in a larger range of the seasonal cycle along the east coast. This alongshore gradient in salinity also has implications for the alongshore gradient in annual sea level, which forms the subject of the following chapter.